Basin Research

IAS EAGE

Basin Research (2010) doi: 10.1111/j.1365-2117.2009.00457.x

Role of the bedrock topography in the Quaternary filling of a giant estuarine basin: the Lower St. Lawrence Estuary, Eastern Canada

Mathieu J. Duchesne,* Nicolas Pinet,* Karine Bédard,* Guillaume St-Onge,†'‡ Patrick Lajeunesse,§ D. Calvin Campbell¶ and Andrée Bolduc*

*Geological Survey of Canada-Québec, Québec, Québec, Canada
†Institut des sciences de la mer de Rimouski (ISMER), Université du Québec à Rimouski, Rimouski, Québec, Canada
‡GEOTOP Research Center, Montréal, Québec, Canada
§Centre d'études nordiques and Département de géographie, Université Laval, Québec, Québec, Canada
¶Geological Survey of Canada-Atlantic, Dartmouth, Nova Scotia, Canada

ABSTRACT

The geometry of estuarine and/or incised-valley basins and their protected character compared with open sea basins are favourable for the preservation of sedimentary successions. The Lower St. Lawrence Estuary Basin (LSLEB, eastern Canada) is characterized by a thick (> 400 m in certain areas) Quaternary succession. High- and very high-resolution seismic reflection data, multibeam bathymetry coverage completed by core and chronostratigraphic data as well as a 3-D seismic stratigraphic model are used to document the geometrical relationships between the bedrock and the Quaternary units of the LSLEB. The bedrock geometry of LSLEB is characterized by two large troughs that are interpreted as resulting mainly from repeated (?) periods of glacial overdeepening of a pre-Quaternary drainage system. However, other mechanisms with complex feedback effects such as differential glacio-isostatic uplift, erosion, sedimentary supply, and subsidence may have contributed to the formation of bedrock troughs. The two large bedrock troughs are mostly filled by ~200 m thick Wisconsinan (Marine Isotopic Stages 2–4) and possibly older sediments. Overlying units recorded the retreat of the Laurentian Ice Sheet during the Late Wisconsinan (Marine Isotopic Stage 2) and estuarine conditions during the Holocene. The strong correlation existing between the bedrock topography and the thickness of the Quaternary succession is indicative of the effectiveness of the LSLEB as a sediment trap.

INTRODUCTION

Existing sequence stratigraphy models for nearshore open marine deposits commonly assume that relative sea-level (RSL) changes are the main driver of sedimentary cycles (Wilgus *et al.*, 1988). This assumption is less obvious in the case of estuarine and/or incised-valley basins because the dominant processes affecting these basins are multiple and a function of interdependent parameters that may vary on timescales as short as 10^3 years. In such elongated basins, the complex interaction of multiple controlling parameters is even enhanced during a glaciation period because external forcing factors such as eustacy, ice-margin location, climate, erosion capacity, sedimentation rate, local subsidence, glacio-isostatic rebound and stress regime are all expected to fluctuate over short periods and have feedback effects that may disrupt equilibrium and force sedimentary adjustment.

Estuarine and/or incised-valley basins are more protected against erosion compared with open sea basins and are more likely to avoid hiatuses in the sedimentary record (Lericolais *et al.*, 2004; Van Andel & Perissoratis, 2006). The effectiveness of such basins in trapping sediments makes them attractive for hydrocarbon exploration (e.g., Allen & Posamentier, 1993; Dalrymple *et al.*, 1994) and to study palaeoclimate evolution (e.g., Mosher & Moran, 2001; Lericolais *et al.*, 2004; Lin *et al.*, 2005; Mallinson *et al.*, 2005; Nordfjord *et al.*, 2005; Rise *et al.*, 2008).

The St. Lawrence Estuary basin (eastern Canada) presents several similarities with incised-valley basins including a great length/width ratio and a well-defined unconformity at its base (Neuendorf *et al.*, 2005). However, the complex and long-term interaction of marine, fluvial and glacial processes in its shaping prevents the use of the incised-valley term and favours a more descriptive classification as an estuarine basin.

Correspondence: Mathieu J. Duchesne, Geological Survey of Canada-Québec, 490 rue de la Couronne, Québec, Canada G1K 9A9. E-mail: mduchesn@nrcan.gc.ca

The St. Lawrence Estuary (Eastern Canada) is one of the world's largest estuarine basins. With dimensions of ~200 × 40 km, the lower Estuary alone (Figs 1 and 2) is ~3 × longer, ~6 × wider and has a Quaternary succession thickness ~14 × greater than the Gironde Estuary (France), one of the most cited Quaternary incised-valleys worldwide (Allen & Posamentier, 1993). The thick sedimentary infill of the LSLEB is mainly attributed to high Early Holocene sedimentation rates driven by the rapid hinterland retreat of the Laurentide Ice Sheet and the large drainage area (~1 × 10^6 km^2) of the basin (St-Onge *et al.*, 2003; Mattheus *et al.*, 2007).

Previous work in the LSLEB have focused on the study of the Quaternary seismic stratigraphic framework (e.g. Syvitski & Praeg, 1989; Massé, 2001; Duchesne *et al.*, 2007), Holocene chronostratigraphic scheme (e.g. St-Onge *et al.*, 2003, 2008) and submarine mass movements (e.g. Duchesne *et al.*, 2003; Campbell *et al.*, 2008; Cauchon-Voyer *et al.*, 2008; Gagné *et al.*, 2009). High-resolution seismic data discussed in the present contribution were briefly presented in Duchesne *et al.* (2007) and used by Pinet *et al.* (2008) to evaluate the hydrocarbon prospectivity of the area. The current paper also includes new seismic stratigraphic interpretations provided by the recent acquisition of very high-resolution seismic reflection data and the generation of a novel basin-scale 3-D seismic stratigraphic model. Through a basin-scale approach, the current study attempts to (1) discuss the different parameters that control the evolution of the bedrock topography in a glaciated and elongated basin, (2) show how bedrock topography is a determinant factor in controlling the distribution and the geometry of the infilling sedimentary units, and (3) investigate the impact of the last glacial episode on the development of the LSLEB.

GEOGRAPHICAL AND GEOLOGICAL BACKGROUND

The St. Lawrence Estuary receives large amounts of freshwater discharge from the Great Lakes and the St. Lawrence River watershed. It opens to the Gulf of St. Lawrence and Atlantic Ocean through the Laurentian Channel, a long and continuous trough > 300 m deep that runs 1500 km from the mouth of the Saguenay River to the edge of the continental shelf in the Atlantic Ocean (Fig. 1). According to Dupuis & Ouellet (1999), dominant winds in the St. Lawrence Estuary blow from the W whereas strongest winds usually gust from the E. Some areas of the Lower St. Lawrence Estuary (e.g. the Manicouagan Peninsula) are exposed to ENE winds which allow the sea to build on a distance of > 350 km and thus induce severe erosion action along this part of the coastline (Fig. 2). Tidal range in the estuary is 2–3 m and tidal currents are up to 3 m s^{-1} (Saucier & Chassé, 2000). The regional hydrodynamic conditions of the estuary are locally modified by several freshwater inputs coming from tributaries of the St. Lawrence River.

The Lower St. Lawrence Estuary Basin (LSLEB) lies in water depths ranging between 0 and 355 m (Fig. 2). The LSLEB is approximately parallel to the Appalachian deformation front. It is wedged between Grenvillian metamorphic rocks in the North and Early Palaeozoic sedimentary rocks belonging to the Appalachians in the South, whereas the major part of the basin floor consists of autochthonous carbonate and siliciclastic rocks belonging to the St. Lawrence Platform (Duchesne *et al.*, 2007; Pinet *et al.*, 2008). Differential erosion has traditionally been considered as the main geological process responsible for the higher relief observed on the north shore, the

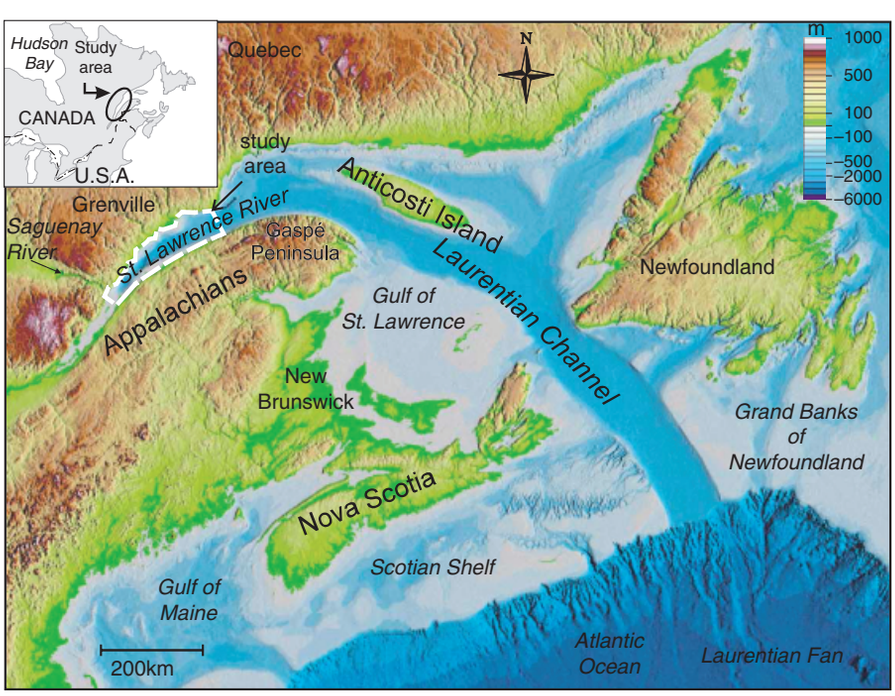

Fig. 1. Geographical setting of the LSLEB. Modified from Shaw *et al.* (2006).

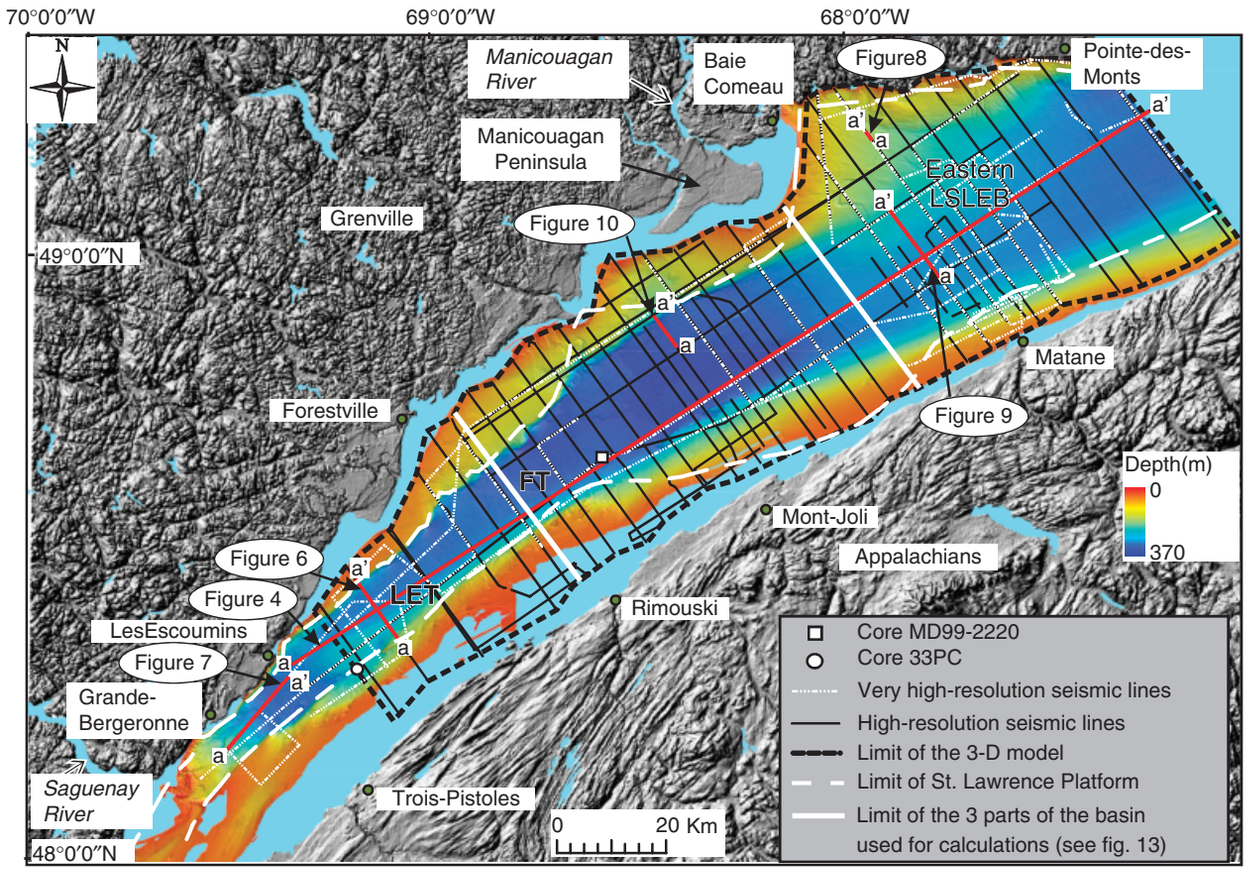

Fig. 2. Multibeam bathymetry of the LSLEB and location of the seismic data sets and cores used in the current study. Figures 4 and 6 to 10 are located. LET = Les Escoumins trough and FT = Forestville trough.

parallelism of the basin with the Appalachian structural grain and the presence of two local bedrock troughs in the LSLEB (i.e. Les Escoumins and Forestville troughs) as softer rocks of the St. Lawrence Platform and the Appalachians have been eroded more easily compared with the more erosion-resistant Grenvillian rocks (Josenhans & Lehman, 1999; Duchesne *et al.*, 2007).

The western part of the LSLEB is characterized by up to 300 m high scarps that bound the Laurentian Channel and correspond to the offshore extent of normal faults mapped on land (Tremblay *et al.*, 2003). These faults exhibit a polyphased deformation history including a middle Palaeozoic episode contemporaneous with the Appalachian Mountains building and an increasingly documented Mesozoic episode (Carignan *et al.*, 1997; A. Tremblay, pers. comm.).

The LSLEB has been greatly influenced by the last glacial cycle (Shaw *et al.*, 2002; Shaw *et al.*, 2006). Recent models based on geological, geochronological and geophysical on-land and offshore data (Josenhans & Lehman, 1999; Shaw *et al.*, 2006) envision the Late Wisconsinan (Marine Isotopic Stages 2–3) as a three-stage history. The early stage which spans the time interval between the maximum ice extent and around 14 kyr BP is characterized by a largely marine based ice-sheet. According to Marshall *et al.* (2000) at the Last Glacial Maximum (~20 kyr BP), the Wisconsinan (Marine Isotopic Stage 2) ice-sheet thickness ranged between 1500 and 2400 m in the LSLEB. During this stage the position of the Laurentian Channel ice-stream remained largely unchanged (Shaw *et al.*, 2006). During the mid-stage, at *ca*. 14–13 kyr BP the ice margins retreated rapidly, ice being removed from the St. Lawrence Gulf and Estuary by calving. Open marine conditions are recorded in the study area at 13.5 kyr BP (Locat, 1977). The late stage, after 13 kyr BP, is marked by largely terrestrial ice sheets for which the retreat is mainly controlled by climatic variables, and not by calving and ice streaming, while a stabilization phase of the Laurentide Ice Sheet in the Laurentian Channel was recorded during the Younger Dryas by the presence of ice-proximal glaciomarine sediments (St-Onge *et al.*, 2008).

During the first millennia following the last glacial retreat, glacio-isostatic rebound was very rapid (3.2 cm yr^{-1} between 13 and 9 kyr BP) inducing a rapid RSL drop of 140 m since the early Holocene (Fig. 3; Dubois, 1980; Dyke & Peltier, 2000; Dionne, 2001). RSL curves from the south shore of the estuary indicate that the rate of emergence strongly decreased after 9 kyr BP to <0.1 cm yr^{-1} at present (Fig. 3; Dionne, 2001).

The Quaternary infill of the LSLEB has mainly been assessed by means of seismic reflection data because

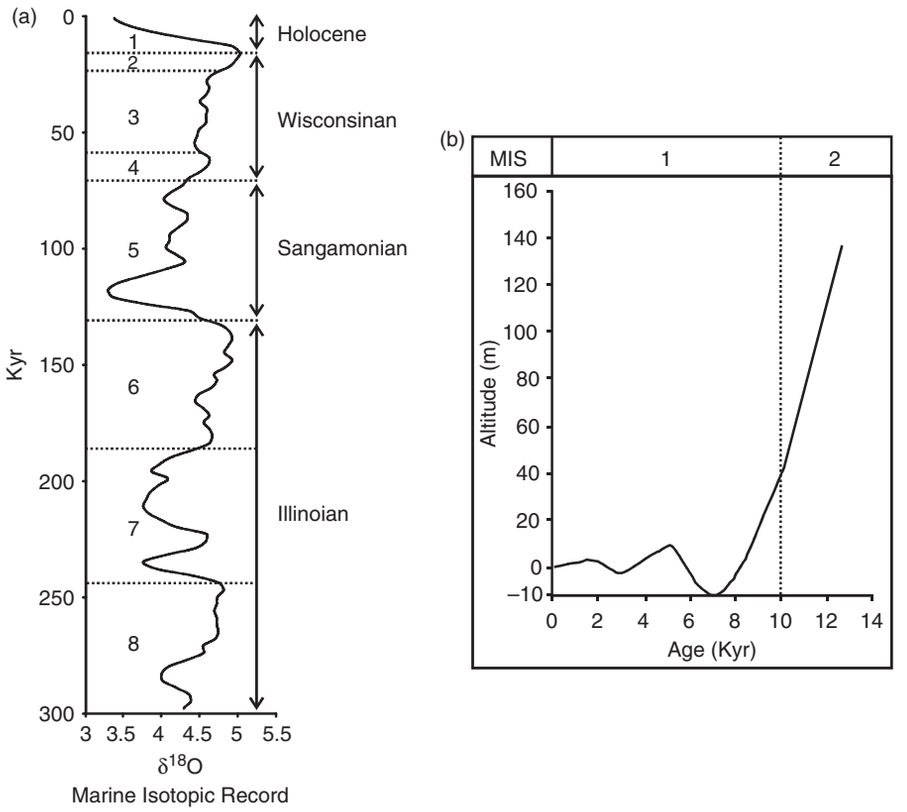

Fig. 3. (a) Marine Isotopic Stages 1–8 curve and corresponding geological epochs. Data courtesy of the Delphi Project (http://www.esc.cam.ac.uk/research/research-groups/delphi/coredata/v677846) (b) Late Quaternary relative sea level curve of the southern shore of the St. Lawrence Estuary (modified from Dionne, 2001). MIS = Marine Isotopic Stage.

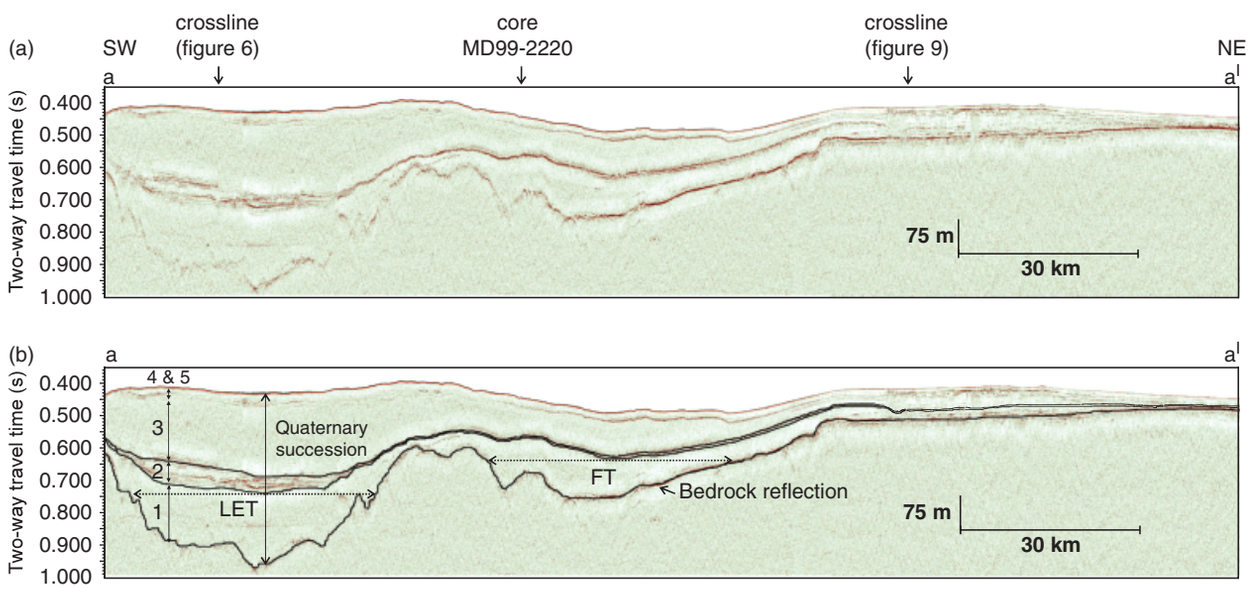

Fig. 4. Along-strike high-resolution seismic section of the LSLEB (see Fig. 2 for location). LET = Les Escoumins trough FT = Forestville trough. Numbers refer to seismic units (Modified from St-Onge *et al.*, 2008).

the important thickness of the sedimentary package (> 400 m in certain areas) makes the totality of the succession impossible to reach with conventional coring devices (Fig. 4; Syvitski & Praeg, 1989; Massé, 2001; Duchesne *et al.*, 2007). Thus, the lithological and geochronological information available in the LSLEB is incomplete (Syvitski & Praeg, 1989; St-Onge *et al.*, 2003, 2008) as the lower part of the Quaternary succession [seismic unit 1 (S1), see below and Fig. 4], which is up to 210 m thick, has never been sampled. Nevertheless, strategic coring operations have detailed the Late Wisconsinan to modern sedimentary succession and permitted to tie the upper seismic package [seismic units 2 (S2)–seismic unit (S5)] with chronostratigraphic data.

MATERIALS AND METHODS

Data sets

High-resolution seismic data consist of 55 single-channel seismic sections, for a total length of >3300 km. High-resolution seismic data were collected with a sparker source (Fig. 2; Duchesne & Bellefleur, 2007). These data have a peak frequency of $\sim$200 Hz and a vertical resolution of 3 m permitting to image the entire Quaternary succession and the topmost portion of the bedrock for a maximal penetration of $\sim$1000 m. Lines were gathered according to a grid oriented northwest–southeast with a spacing between adjacent lines of 2.5, 5 or 10 km tied with five lines oriented perpendicular to the grid [southwest–northeast]. More than 1500 km of very-high-resolution seismic reflection sections were also collected with a Huntec single-channel Deep-Tow-System (Fig. 2; McKeown, 1975). These boomer data have a peak frequency of $\sim$900 Hz, a vertical resolution of 0.8 m and an average penetration of $\sim$125 m. The majority of the 57 Huntec lines were shot according to the high-resolution (e.g. Sparker) data grid permitting to image the architecture of the basin at two different scales. Thicknesses of the units discussed in the text are expressed in metres based on a two-way travel time to depth relationship derived with a velocity of 1520 m s^{-1} that corresponds to the average stacking velocity of the Quaternary succession (Bellefleur *et al.*, 2006). Coverage of $\sim$7700 km^2 of multibeam bathymetry is used in this study (Fig. 2) to provide a complete picture of the seafloor of the study area for water depths >30 m. Pre-2005 data sets were collected with a Simrad EM1000 (Horeton, Norway) echosounder whereas 2005–2007 data sets were collected with a Simrad EM1002 echosounder. Both systems had a peak frequency of 95 kHz. A bathymetric grid of the seafloor which has a 10×10 m planar resolution and a submetric vertical resolution was generated from the data (Fig. 2).

Two piston cores permitted to tie geological information to the regional seismic units (Fig. 2; Duchesne *et al.*, 2007; St-Onge *et al.*, 2008). Core MD99-2220 is 51.6 m long and was raised from the Laurentian Channel. It permitted to assess the Early to Late Holocene stratigraphy and chronology with seven AMS ^{14}C dates (St-Onge *et al.*, 2003). Core 33PC is 8.33 m long and was sampled on the southern shelf. It allowed documenting the Late Wisconsinan and deglaciation history of the basin with four additional AMS ^{14}C dates (St-Onge *et al.*, 2008). For comparison purposes, all ages provided in the paper are conventional ^{14}C ages.

3-seismic stratigraphic model

A 3-D seismic stratigraphic model was generated by using the high-resolution seismic sections. On each section, horizons corresponding to the upper boundary of key seismic units were picked and used to build surfaces with the discrete smooth interpolation (DSI) method (Mallet, 1989; Mallet, 1997). This method allowed using the picks as 'control nodes' and major topographic features parallel to the basin axis acted as 'control curves' to constrain the modelling of the surfaces. The DSI-generated surfaces that are 'as smooth as possible' without violating the constraints imposed by control nodes and curves (Mallet, 1997).

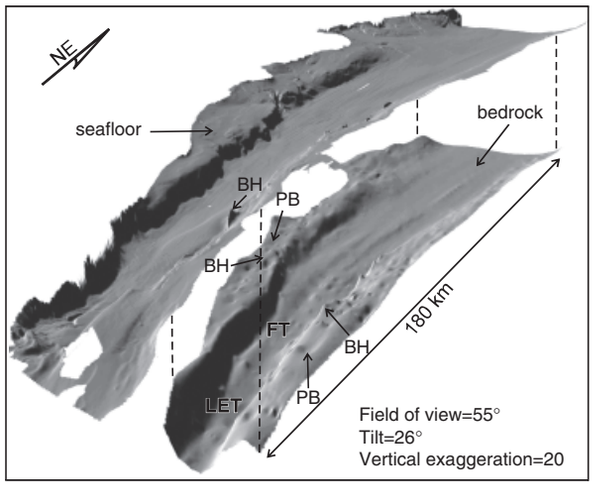

Fig. 5. Perspective view of the bedrock surface extracted from the 3-D seismic stratigraphic model and high-resolution bathymetric imagery of the seafloor. Dashed-lines indicate the extent of the bedrock surface versus the multibeam data coverage. BH = bedrock high, FT = Forestville trough, LET = Les Escoumins trough, PB = ponded-basin.

The resulting surfaces were utilized to create a volume model of 11 520 km^3 ($180 \times 65 \times 1.1$ km) that has horizontal and vertical resolutions of 0.25 and 0.005 km, respectively. This model adequately reflects first-order features such as dip and thickness variations of seismic units. It is also in agreement with more subtle features such as discontinuous bedrock highs outcropping in the LSLEB that have been independently imaged on multibeam bathymetry (Fig. 5). Depth slices and cross-sections were extracted from the 3-D model and volume calculations of the various units were done to improve geological interpretations of the area.

RESULTS

Seismic units

Eight seismic units have been distinguished in the Quaternary succession, five of them being of regional extent. Seismic units 6 (S6), 7 (S7) and 8 (S8) are of local extent and not in stratigraphic order as they can be observed at different positions within the stratigraphy. Seismic units were identified and delimited based on amplitude, morphology of the reflections and geometry of the various seismic bodies in accordance to the method of Sangree & Widmier (1979).

S1

S1 is stratigraphically the lowermost unit and unconformably overlies the bedrock (Figs 4, 6–8 and 10). It has gener-

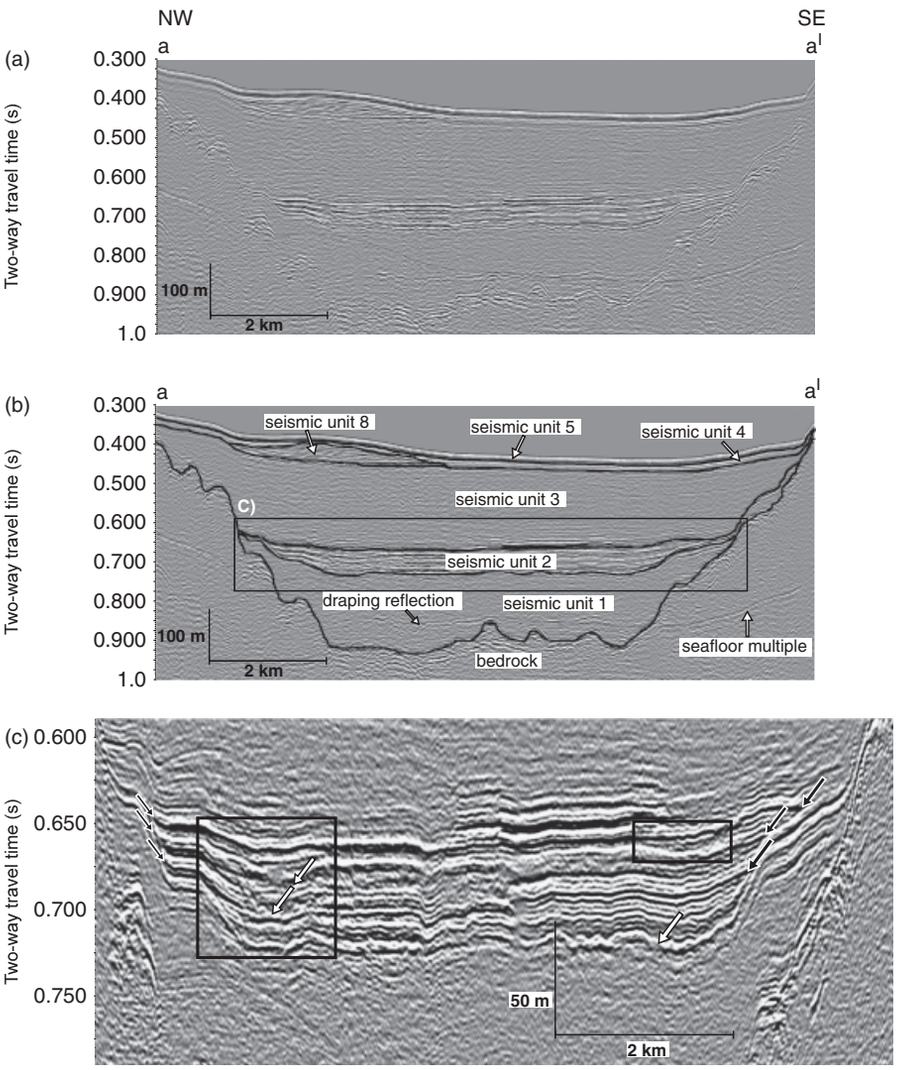

Fig. 6. (a) Uninterpreted and (b) interpreted high-resolution seismic section in the upstream part of the study area. (c) Enlargement of S2 shows a stacked channels complex (left box) and a channel (right box). White arrows denote incisions at the base of two channels and at the lower boundary of S2 whereas black arrows point out the onlapping reflections. See Fig. 2 for seismic section location.

ally a transparent character even though few discontinuous low-amplitude reflections are imaged locally. Its upper boundary corresponds to a high-amplitude reflection that marks the base of the S2. S1 reaches a maximum thickness of 187 m in two troughs located in the SW portion of the LSLEB (see Fig. 2), before thinning considerably to < 5 m in the easternmost part of the study area. Thin (< 30 m) and discontinuous patches of S1 are also present on both shoulders of the Laurentian Channel (Fig. 8).

S2

S2 is characterized by a series of parallel high-amplitude reflections (Figs 4, 6–8 and 10). The seismic character of the reflections changes along-strike of the LSLEB, from flat between the mouth of the Saguenay River and the Manicouagan Peninsula to wavy and even discontinuous until at least the NE-most point of the study area (i.e. Pointe-des-Monts; Figs 2 and 4). S2 is wedge-shaped, having a maximum thickness of 70 m in the SW part of the LSLEB, before diminishing to < 10 m close to Pointe-des-Monts. In most of the Laurentian Channel, S2 drapes unit S1. However, in the southwestern portion of the study area where the steepest bathymetric scarps and the thickest Quaternary succession are located, reflections of S2 have a convex geometry in sections perpendicular to the LSLEB and abut against the upper part of S1 (Fig. 6).

In the upstream part of the surveyed area, channels are observed within unit S2 (Fig. 6c). These features, parallel to the longitudinal axis of the basin, can be traced on $\sim$40 km from Grande-Bergeronne to Forestville (Fig. 2). The most prominent channel complex is positioned along the scarp that defines the NE shoulder of the Laurentian Channel. This channel complex has a width and thickness decreasing north-easterly (respectively, from 3.2 to 1.4 km and from 50 to 45 m) and includes stacked sedimentary bodies that covers the whole unit 2. An erosional contact is locally imaged at the base of stacked sedimentary bodies (Fig. 6c). Another channel is imaged near the southern wall of St. Lawrence Channel in the topmost part of S2 (Fig. 6c). Its width decreases downstream from 1.4 to 1 km whereas it thins in the same direction from 20 to 10 m.

A very high-resolution profile (Fig. 7) extends to the SW of the high-resolution profile shown on Fig. 4 and docu-

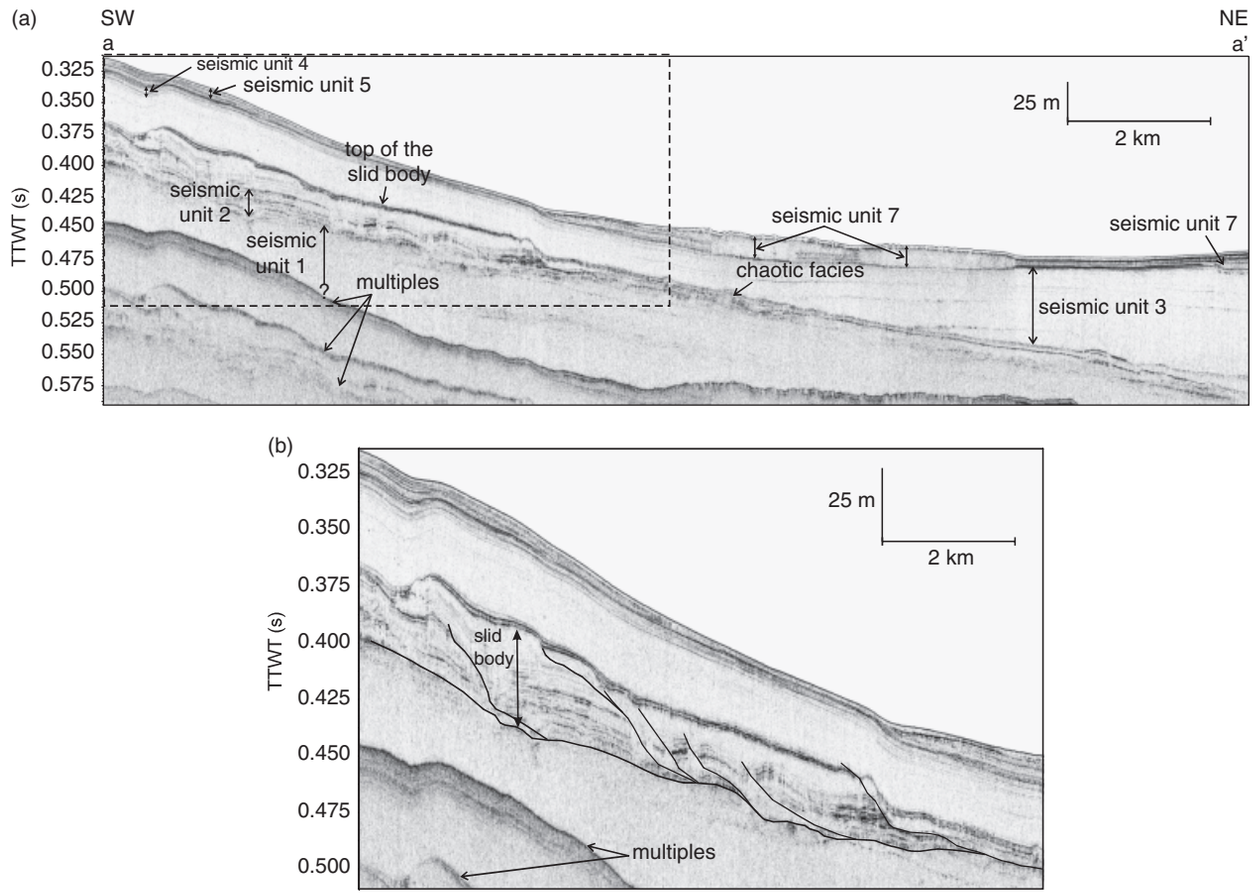

Fig. 7. (a) Interpreted very high-resolution seismic section in the upstream portion of the LSLEB. Dashed-line box denotes the position of the enlarged segment of the line presented in (b) showing the internal architecture of a displaced mass included within S2. Bold arrow in (b) points out the vertical extension of the displaced mass. See Fig. 2 for seismic section location.

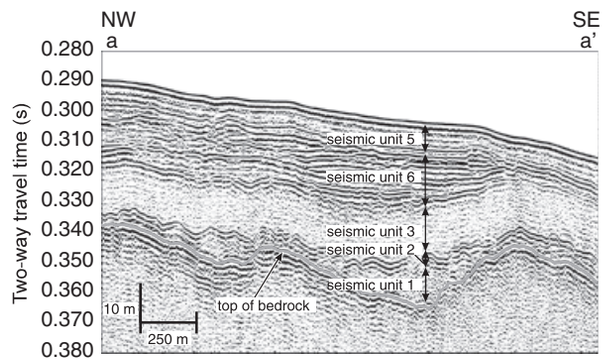

Fig. 8. Interpreted high-resolution seismic stratigraphy included in a small ponded-basin. Note that S1 is thickest in the ponded-basin whereas the thickness of S3 is constant on the section as the signature of the ponded-basin tends to disappear through deposition of S6. See Fig. 2 for seismic section location.

ments the detailed geometry of units 2–5 in the SW portion of the study area. S2 and the basal part of S3 are involved in a landslide deposit. Internally, the slid body is composed of slightly rotated blocks with a basal stratified seismic facies (up to 22 m thick) overlain by mostly transparent reflections with few low-amplitude reflections. A distinctive high-amplitude reflection overlaps the slide headwall scars and marks the top of the slid body (Fig. 7). Chaotic facies are found near the slide toe. Along most of the profile, the slip horizon of the slide exploits the base of the seismically well-stratified interval (S2).

S3

S3 is predominantly transparent with some low-amplitude parallel reflections, few onlaps and several contorted discontinuous reflectors of weak amplitude (Figs 4, 6–8 and 10). It drapes the entire Laurentian Channel and small ponded-basins observed on both shoulders of the LSLEB (Fig. 8). Similarly to S1 and S2, its maximum thickness (190 m) is observed in the SW portion of the LSLEB and decreases gradually to a few metres at the easternmost end of the basin.

S4

Parallel to sub-parallel reflections of low-amplitude constitute S4. In the Laurentian Channel, its thickness varies between $\sim$25 m to the SW and $<$5 m to the NE (Figs 4, 6–8 and 10). At some locations, its lateral extent is abruptly

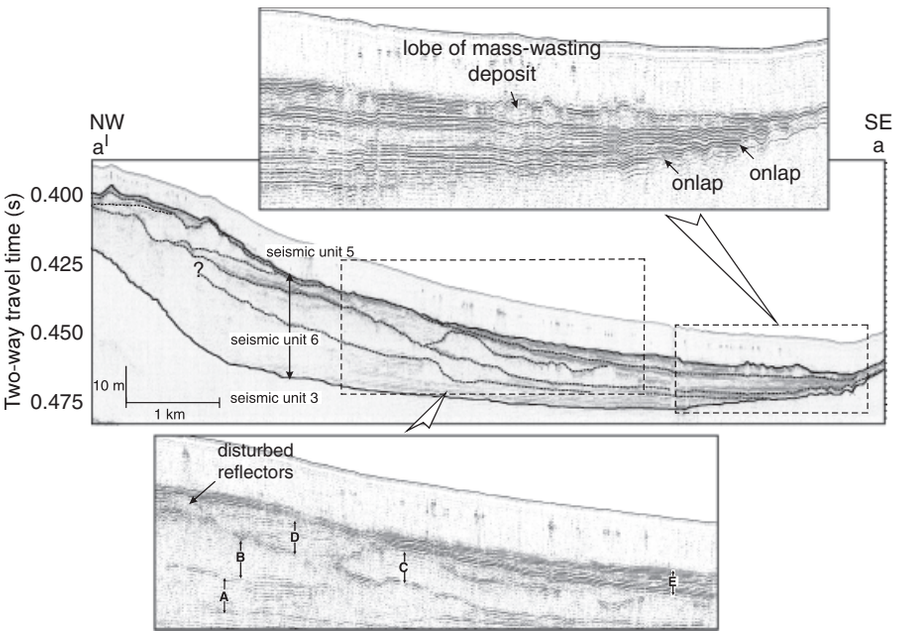

Fig. 9. Interpreted seismic section off the east side of the Manicouagan Peninsula with focus on the internal geometry of S6. Dashed-line boxes indicate the location of the insets on the seismic line showing the complex internal architecture of this unit. See Fig. 2 for seismic section location. Letters A–E refer to seismic bodies that may be distinguished with the S6.

interrupted by seismic units of local occurrence. Unit S4 is also present on both shoulders of the basin.

S5

S5 is formed by low-amplitude reflections parallel to the seafloor (Figs 4, 6–8, 9 and 10). Its thickness is relatively uniform, ranging from 10 to 20 m over the whole surveyed area.

S6

S6 is wedge-shaped, of local lateral extent and includes several sub-units (Fig. 9). Internally, it consists of high- to medium-amplitude flat parallel reflections which are in some cases interrupted by U-shaped features that contain contorted reflections and can reach 70 m in thickness. The only occurrence of S6 is located 15 km off the mouth of the Manicouagan River near Baie-Comeau (Fig. 2) and its distribution in plan view forms a cone-shaped body with a long axis of >40 km striking NW–SE.

S7

S7 comprises both contorted to chaotic low-amplitude reflections and high-amplitude irregularly shaped reflections (Fig. 10). This seismic unit forms several disconnected wedge-shaped bodies mostly located along the northern flank of the Laurentian Channel and has a maximum thickness of 30 m.

S8

S8 is a wedge-shaped unit of local lateral extent having a maximum thickness of 55 m that is only observed $\sim$15 km east off Les Escoumins (Fig. 2). This sedimentary body is 24 km long and 7 km wide and internally formed by medium-amplitude sigmoidal reflections (Fig. 6).

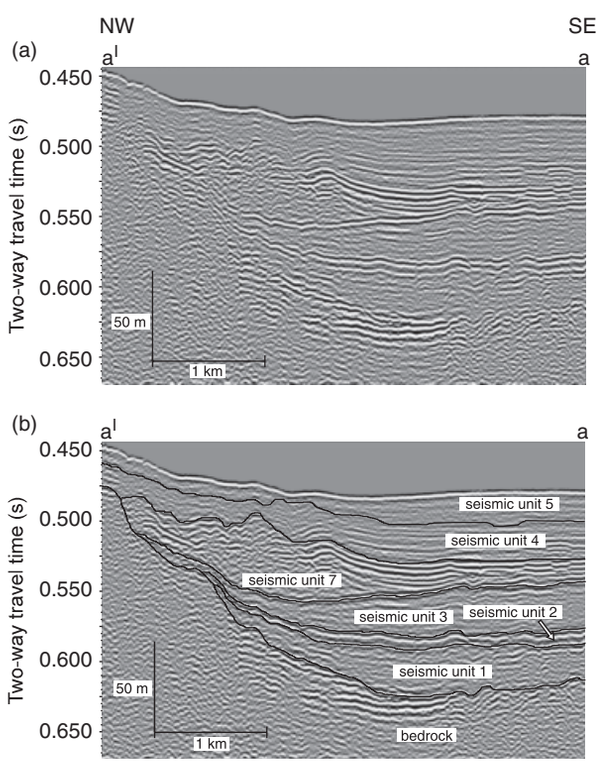

Fig. 10. (a) Uninterpreted and (b) interpreted seismic units in the mid part of the study area with focus on S7. See Fig. 2 for seismic section location.

Correlations between seismic units and core data

To attach a lithological significance to their seismic signature, seismic units S2–S5 were tied to core data. S2 gener-

ally sits between ~250 and ~30 m below the modern seafloor throughout the entire basin. However, it almost outcrops on the southern shelf of the basin where its upper part has been involved in a mass movement (Campbell *et al.*, 2008). At this location (Fig. 2), core 33PC permitted to tie the upper 7 m of S2. The series of parallel high-amplitude reflections characterizing the upper portion of S2 in the SW part of the study area correspond to a glaciomarine succession of a 1.5-m-thick sandy mud facies including ice-rafted debris (ice-proximal deposits) underlying a faintly laminated to homogenous plastic silty clay facies (ice-distal deposits) having a thickness of 5.5 m (Fig. 11; St-Onge *et al.*, 2008). ^{14}C dates obtained in these glaciomarine sediments indicate that part of S2 was deposited between 10 020 and 10 990 yr BP (St-Onge *et al.*, 2008).

Core MD99-2220 (Fig. 2) allowed the upper 30 m of S3 and the entire units S4 and S5 to be tied to sedimentological data. The topmost section of S3, which is characterized by a transparent seismic character and/or by low-amplitude parallel reflections, consists of grey to dark grey laminated clays. For S3, radiocarbon dates of 8730 and 7970 yr BP were, respectively, obtained at a depth of 45 m and at the upper boundary of S3 (14.4 m) (St-Onge *et al.*, 2003). Units S4 and S5 correspond, respectively, to dark grey bioturbated very fine silty clays and fine silty clays (St-Onge *et al.*, 2003; Duchesne *et al.*, 2007). The transition between S4 and S5 has been dated at 7140 yr BP by St-Onge *et al.* (2003).

Interpretation of the seismic units

Seismic interpretation of the different units is based on their reflection characteristics and the core data. Units S1 and S8 are interpreted solely from their reflection characteristics and their position within the basin because they have not been reached by piston cores.

In the marine environment, coarse glacial deposits, such as till, are characterized in seismic records by a chaotic internal configuration or the absence of stratification and by their stratigraphic position below glaciomarine sediments (e.g., King, 1993; Larsson & Stevens, 2008). Unit S1 follows these general characteristics as it is mostly transparent and located below glacio-marine sediments (i.e. unit S2). However, S1 is unusually thick (up to 187 m) compared with well-documented marine till bodies. Moreover, as noted by Syvitski & Praeg (1989), unit S1 is

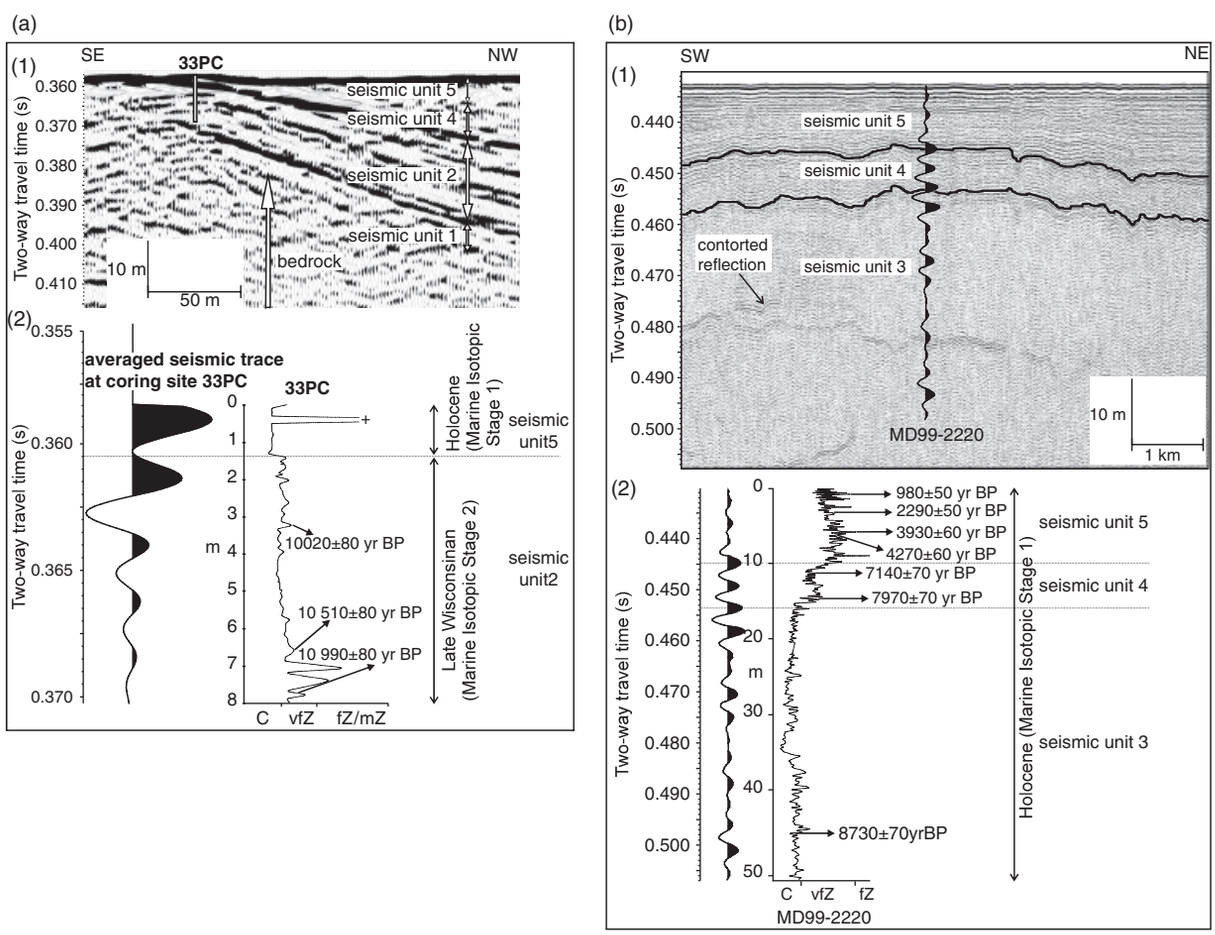

Fig. 11. (a) Correlation between very high-resolution seismic data and core 33PC. (1) Core 33PC plotted on the seismic section. (2) Averaged seismic trace at the coring site tied to the grain-size curve of core 33PC. (b) Correlation between very high-resolution seismic data and core MD99-2220. (1) Synthetic seismogram plotted on the seismic section. (2) Synthetic seismogram tied to the grain-size curve of core MD99-2220. See Fig. 2 for cores location. C, clay; vfZ, very-fine silt; fZ, fine silt; mZ, medium silt.

the thickest where the troughs are the deepest, which is the opposite of what would be predicted for till that is deposited predominantly where basal shear stress decreases.

The generally transparent aspect with only a few low-amplitude discontinuous reflections of S1 suggests the presence of a fairly homogenous deposit formed by a single lithology or multiple lithologies that have been remoulded by strong post-depositional processes such as debris flows (Sangree & Widmier, 1979).

Considering the above-mentioned seismic reflection characteristics, the glacial context of the LSLEB and the age of the overlying units, it appears very likely that unit S1 has been influenced by glacial processes during one or several glacial episode(s). Nevertheless, in the absence of a geochronological tie with unit S1, it remains unclear whether (1) pre-Wisconsinan sediments also compose this unit and (2) pre-Wisconsinan sediments (if present) have been remoulded by glacially induced high-energy processes such as slumping and high-density currents that occurred along the glacier margin leading to remoulding and homogenization with Wisconsinan deposits (Lyså & Vorren, 1997). Nevertheless, till may be present as thin layers or discontinuous patches that cannot be resolved by the resolution of the seismic data (Larsson & Stevens, 2008).

Unit S2 is the deepest core-controlled unit (St-Onge *et al.*, 2008). This unit S2 is the most widespread and easily recognizable seismic unit. Its reflection pattern is most likely generated by a decrease through time in the percentage of sand and by the presence/absence of ice-rafted-debris within the unit. These variations are interpreted by St-Onge *et al.* (2008) as a change from glaciomarine ice-proximal to glaciomarine ice-distal settings. The upper part of unit S2 was most likely formed by the discharge of sediment plumes into the estuary near the glacier termini, the top of the unit being deposited when the front of the glacier was located at ~30 km north from the north shore of the study area (Fig. 12b; Shaw *et al.*, 2002). The decrease in sand and ice-rafted debris content indicates the northern retreat of the Laurentide Ice Sheet during deglaciation (Syvitski, 1989; Vincent, 1989). The thickness of unit S2 strongly decreases towards the NE suggesting that the sediment source was located towards the SW. The seismic signature of channels in the Les Escoumins trough gradually fade out ~30 km downstream from Les Escoumins is another indication that the thickness of S2 at this location is related to its proximity from sediment sources. Moreover, changes of the reflection character of the topmost part of unit S2, from flat to incised, have been correlated with intense iceberg scouring that occurred in the NE part of the LSLEB (Fig. 12b; St-Onge *et al.*, 2008). The absence of an incised seismic signature south of the Manicouagan Peninsula is explained by the greater accommodation space in the Les Escoumins and Forestville troughs at the time the topmost portion of S2 was deposited, the RSL being ~80 m higher than it is today (Dionne, 2001). This suggests that in the SW part of the study area the seafloor was deep enough to remain undisturbed by the keel of the icebergs that were detaching from the retreating ice front. Although the base of unit S2 has not been cored, its onlapping and depression-infilling reflection character indicates that deposits were predominantly transported over the bed probably from the grounding line by either density flows and/or turbidites (Laberg & Vorren, 2000; Mohrig & Marr, 2003).

The predominantly transparent aspect of unit S3 is supportive of a sedimentary body formed by homogenous material (Sangree & Widmier, 1979). Correlation with core MD99-2220 shows that unit S3 corresponds to massive clays deposited by suspension during a period of very high sedimentation rates driven by meltwater discharge from the retreating Laurentide Ice Sheet. At the time of deposition of this unit, the ice front was located ± 200 km north from the north shore of the study area (Shaw *et al.*, 2002) suggesting that sediments were transported to the LSLEB by rivers (Fig. 12c). The occurrence of contorted discontinuous reflections of weak amplitude sparsely distributed over the entire surveyed area between the upper boundary of unit S2 and the middle of unit S3, suggest the formation of debris flow deposits (Fig. 12c; Laberg & Vorren, 2000). This portion of the Quaternary succession is constrained by radiocarbon dates of 10 020 yr BP (top of unit S2) and 8730 yr BP (middle of unit S3). In the study area, maximum glacio-isostatic rebound occurred between 11 000 and 8000 yr BP with average annual rates ranging from 94 to 47 mm yr^{-1} (Dionne, 2001; Bernatchez, 2003). Campbell *et al.* (2008) and Cauchon-Voyer *et al.* (2008) suggested that earthquakes have most likely triggered many submarine slides during this period of significant crustal readjustment leading to the ubiquitous deposition of mass wasting deposits observed within unit S3 (Fig. 12c).

The parallel to subparallel low-amplitude reflections of unit S4 suggest the deposition of contrasting geological layers such as the sedimentation of hemipelagic material (Stow & Piper, 1984; St-Onge *et al.*, 2003; Duchesne *et al.*, 2007). ^{14}C dates suggest that these conditions prevailed over the entire basin for ~800 yr, i.e. between 7970 and 7140 yr BP when the distance to glacier front was more than 250 km north of the north shore (Shaw *et al.*, 2002).

Deposition of hemipelagic sediments is also proposed to explain the low-amplitude reflections parallel to the seafloor forming unit S5. The transition between those two units corresponds to an increase in grain size correlated with a RSL lowstand which was ~10 m below the modern sea level between 7000 and 6000 yr BP (Figs 3 and 12d; Dionne, 1988).

Unit S6 is interpreted as a submarine fan system on the base of its wedge-shaped geometry, the complexity of its reflection pattern, its downlapping internal configuration and its spatial relationship with the Manicouagan River (Figs 2 and 12c). Furthermore, from this perspective, the U-shaped, contorted and high-amplitude reflections observed within unit S6 are interpreted as channels, slumps and/or sand sheets, also described in other well-documented submarine fans (e.g., Berryhill *et al.*, 1986;

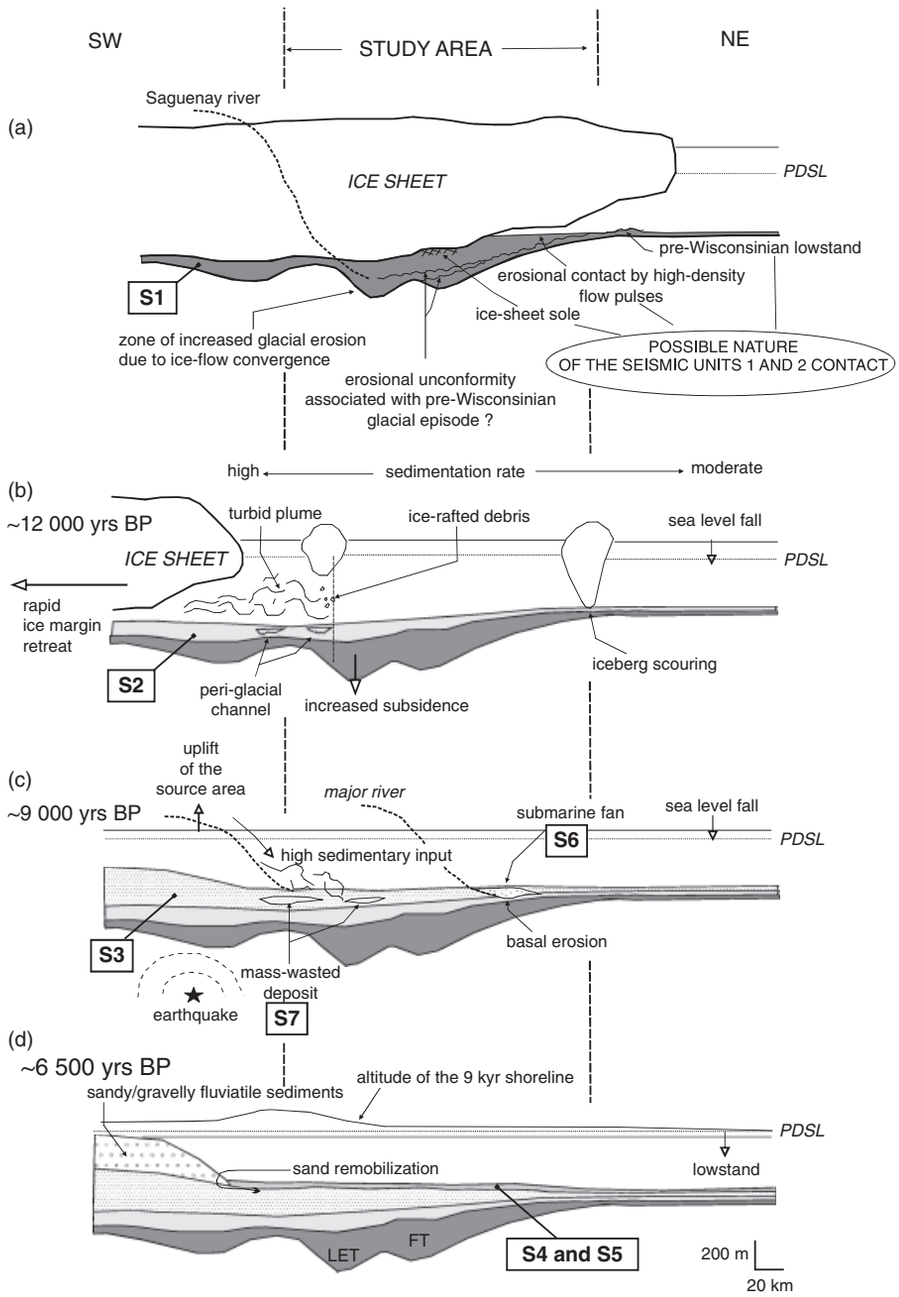

Fig. 12. Schematic longitudinal sections showing the evolution of the LSLEB. (a) sketch illustrating the geometry of unit S1 and three non-exclusive interpretations of the S1–S2 boundary. The influence of ice-flow convergence on glacial erosion rate is schematically illustrated as well as the possibility that the S1 comprises several sedimentary packages bounded by unconformities. (b–d) Show variations of dominant sedimentation mechanisms trough time. During stage b (~12 000 yr BP), the ice margin retreated rapidly, ice being removed from the LSLEB by calving. In the study area, ice-proximal glaciomarine sediments formed by discharge of sediment plumes were deposited (S2). Wavy reflections at the top of the S2 in the NE part of the LSLEB are attributed to intense iceberg scouring. During the stage c (~9000 yrs BP), rapid glacio-isostasic rebound contributed to the uplift of the source area. In the LSLEB, S3 attests of high sedimentation rates driven by meltwater discharge coming from major rivers. Intense seismic activity during this period most likely triggered submarine slides. Schematic representation of S6 and S7 on the sketch corresponding to stage c does not bear any chronological significance. During stage d (~6500 years) an increase in grain size at the base of the S5 is attributed to a RSL lowstand which was ~10 m below modern sea-level. Vertical exaggeration is ~100. PDSL, present day sea level; LET, Les Escoumins Trough; FT, Forestville Trough. S1–S7 refer to S1–S7.

Fulthorpe *et al.*, 2000; Gee *et al.*, 2001; Hjelstuen *et al.*, 2004). Some of these features are presented on Fig. 9 as seismic bodies labelled from A to D and are interpreted as slumps. Seismic body E is interpreted as a high-amplitude-reflection package most likely associated with the deposition of sand sheets (Popescu *et al.*, 2001; Schwenk *et al.*, 2005).

The seismic signature of unit S7 is typical of mass-wasted sediments deposited by debris flows (Sangree &

Widmier, 1979; Laberg & Vorren, 2000). Several papers have already identified the presence of such deposits at various stratigraphic levels in the LSLEB (Syvitski & Praeg, 1989; Massé, 2001; Duchesne *et al.*, 2003; Campbell *et al.*, 2008; Cauchon-Voyer *et al.*, 2008; Gagné *et al.*, 2009). A study by Campbell *et al.* (2008) suggested that a number of factors could have contributed to the formation of mass-wasting deposits such as earthquakes, shallow gas, high sedimentation rates and steep bedrock slopes located on the flanks of the Laurentian Channel. In a detailed study undertaken ~10 km SW of the Manicouagan Peninsula by Cauchon-Voyer *et al.* (2008), two historical earthquakes (i.e. AD 1663 and AD 1860 or 1870) are cited as triggering mechanisms for the sedimentation of mass-wasting deposits. Even if most of the mass-wasting deposits observed in the present study are older than four centuries of seismological records, earthquakes provide one of the preferred triggering mechanisms to explain the presence of mass-wasting deposits within the Quaternary stratigraphy (Fig. 12c).

The mounded and elongated geometry of unit S8 along with its sigmoidal internal reflection configuration and its location parallel to the southern flank of the Laurentian Channel, are indicative of a contourite deposit (Faugères *et al.*, 1999). The strong tidal currents and the existence of internal waves in the SW region of the LSLEB are favourable for the formation of such deposits (Mertz & Gratton, 1995; Saucier & Chassé, 2000; Bolduc & Duchesne, 2009).

3-seismic stratigraphic model observations

For visualization purposes of the model, seismic units S1 and S2 were merged together; this is also the case for units S4 and S5 (Fig. 13). Based on ties done between core and seismic data, the unit corresponding to S1 and S2 is labelled 'Pre- to Early Holocene (including ice-proximal to

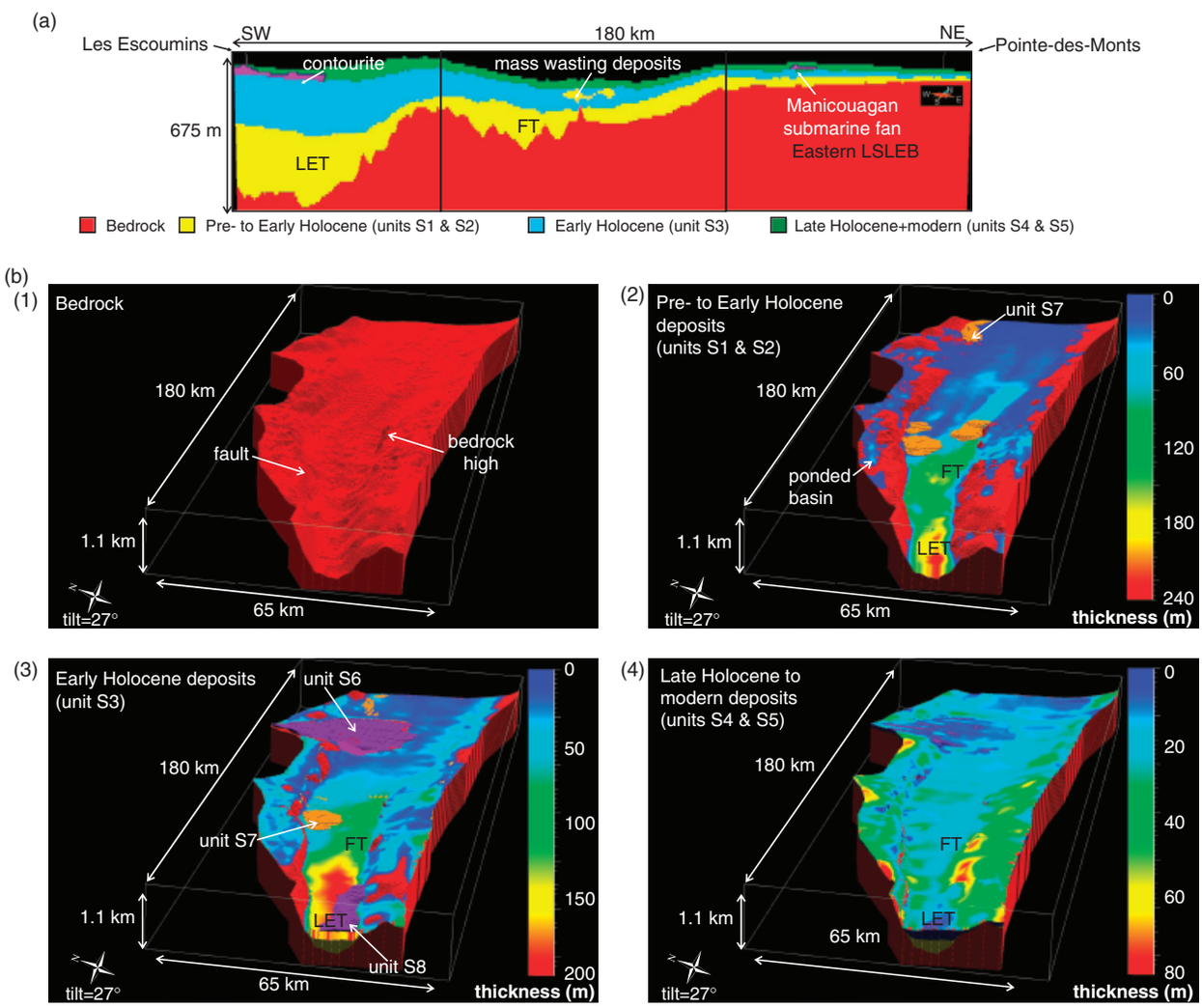

Fig. 13. 3-D seismic stratigraphic model of the LSLEB. (a) Section extracted from the model in the middle of the basin showing the limits of the three parts of the basin used for calculations. Results are listed in the Table 1. LET, Les Escoumins trough and FT, Forestville trough. (b) Model of the basin showing bedrock topography (1), thicknesses of pre- to Early Holocene deposits (2), of Early Holocene deposits (3), and of Late Holocene to modern deposits (4). See Fig. 2 for model location.

ice-distal glaciomarine sediments)', unit S3 'Early Holocene (ice-distal glaciomarine)' and the unit equivalent to S4 and S5 'Late Holocene to modern (post-glacial)'. For volumetric calculations, the model has been split in three areas (Fig. 13 and Table 1). The emphasis has been put on sedimentation rate variations rather than on their relationship with erosion rates because these latter are difficult to quantify regionally and are expected to fluctuate over short periods during a glacial cycle (Ballantyne, 2002).

Bedrock topography

The LSLEB bedrock topography grossly mimics the present day bathymetry. It consists of a steep-walled valley in the south-west that gradually becomes smoother and wider towards the north-east end of the study area with the northern flank usually steeper than the southern flank (Fig. 5). Bedrock still outcrops today in the steeper portions of the basin (Fig. 13b).

Two major troughs are located in the SW portion of the LSLEB. The Les Escoumins trough is 47 km long, 8.5 km wide and ~300 m deeper than the surrounding bedrock with bordering slopes of 1° and 0.6°, respectively, on the NW and SE side of the trough (Figs 4, 5 and 13). The Forestville trough is 54 km long, 10.5 km wide and ~190 m deeper than the neighbouring bedrock and bounded by slopes of 0.2°–0.4° (Figs 4, 5 and 13).

In the SW part of the LSLEB, the SE shoulder of the Laurentian Channel is characterized by a series of bedrock highs representing the limits of small ponded basins that are sparsely distributed over ~100 km (Figs 4, 5 and 13). These ponded basins stand at ~100 m below sea level and have average length and width of 2 and 1.4 km, respectively. The northern shoulder of the Laurentian Channel is also characterized by ponded basins bounded by steep bedrock highs (Figs 4 and 13). In cross-section, bedrock highs are disposed in a stair-like fashion having a length of a few to 10 km, a width of 1.5–2 km and height of 30–40 m.

Pre- to Early Holocene

Based on calculations that included seismic units of both regional and local extent, the total volume of Quaternary sediments in the LSLEB is estimated to 1.2×10^{12} m^3. The volume of pre- to Early Holocene deposits is 354×10^9 m^3 and represents 29.5% of the total Quaternary succession (Fig. 13 and Table 1). The largest volume of pre-Holocene deposits is observed in the two bedrock troughs as 130×10^9 and 150×10^9 m^3 of sediments, respectively, fills the Les Escoumins and the Forestville troughs (Fig. 13). NE of the Forestville trough, the volume of this unit significantly decreases to 74×10^9 m^3 as the basin widens. Pre- to Early Holocene deposits are also included within the ponded basins over the whole area (Fig. 13b). The normalized thickness (i.e. the ratio between the volume of deposits and the surface of the basin or part of the basin) of Pre- to Early Holocene deposits in the Les Escoumins trough is almost twice of what is observed in the Forestville trough and nearly 4 times thicker than Pre- to Early Holocene deposits included in the Eastern LSLEB (Table 1).

Early Holocene

The largest volume of sediments corresponds to Early Holocene deposits with 39.25% (471×10^9 m^3) of the total volume (Table 1). These deposits significantly contributed to reduce the topographic expression of the Les Escoumins and the Forestville troughs. They fill 44% (186×10^9 m^3) of the Les Escoumins trough and 37% of both the Forestville trough and the Eastern LSLEB (Fig. 13 and Table 1). On the shelves, Early Holocene sediments contributed significantly to the filling of the small ponded basins. This succession also includes unit S6 and several seismic bodies corresponding to unit S7. The normalized thickness of Early Holocene deposits in the Les Escoumins trough is more than two times thicker than the equivalent deposits contained in the Forestville trough and three times thicker than Early Holocene deposits enclosed in the Eastern

Table 1. Volume calculations computed from the 3-D seismic stratigraphic model

Part of the basin	Parameter			
	Les Escoumins trough	Forestville trough	Eastern LSLEB	LSLEB
Length (km)	50	68	62	180
Maximum width (km)	37	46	55	55
Surface (m^2)	1.4×10^9	2.8×10^9	2.8×10^9	6.8×10^9
Volume of Pre-to Early Holocene deposits (m^3)	130×10^9	150×10^9	74×10^9	354×10^9
Normalized thickness of Pre-to Early Holocene deposits (m)	93	54	26	52
Volume of Early Holocene deposits (m^3)	186×10^9	167×10^9	118×10^9	471×10^9
Normalized thickness of Early Holocene deposits (m)	133	60	42	69
Volume of Late Holocene to modern deposits (m^3)	97×10^9	125×10^9	89×10^9	311×10^9
Normalized thickness of Late Holocene to Modern deposits (m)	69	45	32	46
Total volume of Quaternary sediments (m^3)*	423×10^9	453×10^9	322×10^9	1.2×10^{12}
Normalized thickness of Quaternary sediments (m)	302	161	115	176

*Includes seismic units of local extent, i.e. seismic units 6, 7 and 8.

LSLEB (Fig. 13 and Table 1). The Forestville trough exhibits normalized sedimentary thicknesses that are slightly lower (for the Early Holocene and Late Holocene to modern periods) than for the entire basin. This is caused by the reduced accommodation space of the Forestville trough compared with the Les Escoumins trough as it became an inefficient sediment trap throughout the Early Holocene.

Late Holocene to modern

Late Holocene to modern deposits conformably overlie Early Holocene sediments (Fig. 13b). They represent 26% ($311 \times 10^9\,m^3$) of the total volume of the Quaternary succession. The smallest percentage (29%) is found in the Eastern LSLEB which is contrasting to the NE decrease in volume of Early Holocene deposits. The normalized thickness of Late Holocene to modern deposits in the Les Escoumins trough is 1.5 times thicker than deposits of same age included in the Forestville trough and twice thicker than Late Holocene to modern deposits contained in the Eastern LSLEB.

Major changes in sedimentation rates between Early Holocene and Late Holocene

Based on volume calculations computed from the model and dates available from core MD99-2220, volumetric rates of sedimentation were calculated for Early Holocene and Late Holocene to modern deposits. Since the deepest date for Early Holocene deposits is ~49 m above the base of this unit, the age of the base was extrapolated using a constant sedimentation rate.

The volumetric rate of sedimentation for Early Holocene in the LSLEB is $2.4 \times 10^8\,m^3\,yr^{-1}$ whereas it is $3.9 \times 10^7\,m^3\,yr^{-1}$ for Late Holocene to modern deposits. This difference of approximately one order of magnitude between those two periods supports the idea of a drastic change of sedimentation in the LSLEB that occurred ~7970 yr BP, i.e. the approximate chronological limit between Early Holocene and Late Holocene to modern deposits.

DISCUSSION

Processes controlling bedrock morphology

In most (if not all) published studies, the morphology of the bedrock in the LSLEB has been loosely attributed to glacial overdeepening of a pre-existing drainage system (Nota & Loring, 1964; Syvitski & Praeg, 1989; Martineau & Hocq, 1994; Josenhans & Lehman, 1999; Shaw *et al.*, 2002, 2006; Dyke, 2004). This interpretation was mostly based on the U-shaped geometry in cross-section of the SW segment of the LSLEB and on onshore ice-motion indicators showing that the Lower St. Lawrence Estuary acted as the main ice-stream in SE Canada during, at least, the Wisconsinan glacial episode (Parent & Occhietti, 1999). The longitudinal profile of the LSLEB tends to support this interpretation as the bedrock surface is punctuated by several steps and overdeepenings of hundred metres deep (i.e the Les Escoumins and Forestville troughs) similar to those of glacial valleys, a characteristic that contrasts with the generally smooth longitudinal profiles of fluvial valleys.

Considering rates of glacial erosion beneath ice-streams ($> 1\,mm\,yr^{-1}$; Bougamont & Tulacyk, 2003) the depth of overdeepenings in the LSLEB (up to ~300 m compared with surrounding bedrock; ~800 m compared with actual sea-level) is probably too high to result from a single episode of glacial erosion, and thus their presence suggests they result from several periods of bedrock incision (Nota & Loring, 1964). As noted above, it is unclear if the sedimentary remnants of each erosion episodes have been preserved within unit S1 (Fig. 12a) or if they have been washed away during the last glacial episode.

In the LSLEB, two main parameters may have enhanced the differential glacial erosion of the bedrock. First, the Les Escoumins and Forestville troughs are both hosted by rocks of the St. Lawrence Platform (Pinet *et al.*, 2008). This geological domain is formed by rocks that are easy to erode compared with the surrounding Grenvillian and Appalachian rocks. Second, tributaries of the palaeo St. Lawrence River may have significantly modified the dynamics of Quaternary ice streams. The Saguenay Fjord (Fig. 1) a 90 km long, steep-sided trough included within the Saguenay graben (e.g., Syvitski & Praeg, 1989; Syvitski & Schafer, 1996), consisting in a major ice-stream probably influenced glacial erosion within the Laurentian Channel (Fig. 12a, Dionne, 1973; Lasalle & Tremblay, 1978; M. Parent, pers. comm.). Numerical simulations performed by MacGregor *et al.* (2000) reveal that overdeepening in the trunk valley can be attributed to the increase of the ice discharge below a tributary junction. As noted by MacGregor *et al.* (2000), multiple tributaries could explain multiple valley overdeepenings. However, in the case of the LSLEB, it is unclear if the Les Escoumins and Forestville troughs were formed in response to perturbations associated to two tributaries or if they correspond to a single composite trough divided by a more resistant sill.

Several studies (e.g., Small & Anderson, 1998; Meigs & Sauber, 2000; Montgomery & Greenberg, 2000; Pelletier, 2004; Stern *et al.*, 2005; Champagnac *et al.*, 2007; Medvedev *et al.*, 2008; Pelletier, 2008) document that the isostatic response of localized glacial erosion (in valley) leads to regional (within a ~100 km wide region) uplift, causing some peaks to increase elevation. In southern Québec, such a process of glacio-isostatic relief production may explain the elevation of high peaks (up to 1181 m) on the northern shore of the St. Lawrence River close to the Saguenay River. Glacio-isostatic relief production is expected to have its own effects on climate, ice stream dynamic, erosion and sediment supply.

Arguments presented above suggest that differential glacial erosion enhanced by the presence of relatively soft rocks (St. Lawrence platform) and of major tributaries is the main process that led to the observed bedrock mor-

phology. Other processes with complex feedback effects, including differential glacio-isostatic uplift (Dyke & Peltier, 2000), erosion, sedimentary supply, and subsidence caused by both glacial and sediment loading may also have played a role in the shaping of the LSLEB.

Role of the bedrock topography on the basin fill

Bedrock topography controls the architecture of Quaternary deposits in the LSLEB. Strong correlation exists between the thickness of the Quaternary succession and the bedrock topography as both the depth-to-bedrock and the Quaternary sediment thickness decrease toward the NE. Between Marine Isotopic Stages 4 and 1, the Les Escoumins and Forestville troughs most likely contributed to prevent a large quantity of sediments coming from the head of the Laurentian Channel from being deposited downstream and to reach the termini of the system, the Laurentian Fan.

The influence of the bedrock topography on the Quaternary filling of the basin tends to decrease over the Holocene. In particular, the imprint of the Les Escoumins and Forestville troughs has considerably faded since the Middle Holocene even if today the morphology of both troughs is still recorded on the basin floor. The present-day signature of Les Escoumins trough on the seafloor is less apparent than the signature of the Forestville trough (Fig. 4) because the former was located in the narrowest part of the LSLEB and closer to major sedimentary sources such as the front of the Laurentide Ice Sheet, and for these reasons it has accommodated a larger volume of material.

On the northern shelf, the bedrock morphology is controlled in part by inherited normal faults (Lamontagne *et al.*, 2003) or/and by a cuesta-like morphology (Pinet *et al.*, 2008) that played a role of barrier disabling sedimentary bypass from the shelf to the basin floor for sediments transported along the seabed. In bedrock lows, the trapping of sediments coming from tributaries of the St. Lawrence Estuary was enhanced, leading to the formation of small depocenters. It is only when the bedrock lows are filled that sedimentary bypass to the basin floor is restored. Most of the ponded basins were completely filled between the Holocene and today. However, some remain effective sediment traps on the southern shelf between the SW end of the study area and Mont-Joli (Fig. 2).

Seismic data suggest that bedrock topography is not the main parameter that controlled the mode of deposition of the various units of regional extent, although it controlled their geometry. However, deposition of S7 and S8 has been influenced by the local topography of the bedrock. The presence of mass-wasting deposits (unit S7) is strongly correlated with the steepness of the bedrock walls on the northern flank of the valley over the entire basin and on the southern flank of the basin in its SW segment (Syvitski & Praeg, 1989; Duchesne *et al.*, 2003; Campbell *et al.*, 2008; Cauchon-Voyer *et al.*, 2008). Steep bedrock walls bordering the basin act as a major predisposing factor that restricts the deposition of thick sediment accumulation, since one of the parameters controlling failure initiation is the critical angle of repose of the material, which is attained more rapidly on steeper slopes (Bromhead, 1986). Unit S8 is observed in an area where the Laurentian Channel is narrow and bedrock walls are steep on the northern flank. Bedrock topography influences water-mass circulation and causes a bottleneck effect that locally increases the velocity of the tidal currents on the northern flank of the channel, favouring the formation of a coutourite deposit on the southern flank (Faugères *et al.*, 1999).

Significance of seismic unit boundaries

S1-S2

Two end-member scenarios may be envisioned to explain the origin of unit S1 sediments: (1) the Wisconsinan Laurentide Ice Sheet eroded and evacuated the entire sedimentary succession previously deposited in the St. Lawrence Estuary or (2) remnants of older glacial and interglacial episodes are preserved at the base of the sedimentary succession (Occhietti *et al.*, 1995; Massé, 2001). Depending on the scenario, the significance of the S1–S2 boundary changes dramatically and it may represent variation in the sedimentation without significant hiatus or the sole marking of the Late Wisconsinan Laurentide Ice Sheet advance.

The seismic reflection characteristics of units S1 and S2 imply that both units were deposited under very different sedimentary conditions. The presence of channels incised through unit S2 suggests that erosion by water occurred during its deposition. Since units S1 and S2 are trapped in ponded basins on the northern and southern shelves of the basin, it is possible that these depressions efficiently protected both units from being eroded from lowstands that followed the deposition (Dionne, 1988).

Over most of the LSLEB, S2 gently drapes S1. The draping internal geometry of S2 shows that its deposition contributed to erase the remnant morphology of the bedrock that was still recorded at the top of S1 in the Laurentian Channel. Interestingly, in the narrowest part of the basin where unit S2 is the thickest (SW-most part of the study area), the upper limit of unit S1 pinches higher up on the sides of the basin than the top of unit S2 (Fig. 6). This most likely indicates that the upper boundary of S1 corresponds to an unconformity. This surface either represents a pre-Wisconsinan lowstand or submarine incision that occurred near the glacier termini by high-density flow pulses or the base of the Late Wisconsinan Laurentide Ice Sheet (Fig. 12a). Since the time hiatus, if any, between unit S1 and S2 is unknown, it leaves the three hypotheses open to discussions (St-Onge *et al.*, 2008).

S2–S3

The geological significance of the S2–S3 boundary has been attributed by St-Onge *et al.* (2008) to local readvances

or stillstands of the Laurentide Ice Sheet margins in the marine environment during the Younger Dryas (i.e. the Goldthwait Sea; see Dyke & Prest (1987) and Lapointe (2000)). On the eastern Scotian Shelf, King (1994) documented Younger Dryas sediments having the same seismic and lithological characteristics as the top of unit S2. Since this boundary is recognized over the entire LSLEB, in the Gulf of St. Lawrence (see St-Onge *et al.* 2008) and most likely down to the Scotian Shelf, it strengthens the possibility that it is linked to a large-scale event.

S3–S4

The S3–S4 boundary is correlative with the base of unit 2 of St-Onge *et al.* (2003). It is attributed to a significant reorganization of the Laurentide Ice Sheet meltwater drainage pathways that occurred ~7700 yr BP induced by the rapid collapse of ice in Hudson Bay (Fig. 1). This event led to the catastrophic drainage of glacial lakes Agassiz and Ojibway into Hudson Strait, therefore diminishing meltwater discharge through the St. Lawrence Estuary and resulting in a drastic decrease in sedimentation rates (see above results in *Major changes in sedimentation rates between Early Holocene and Late Holocene*; Fig. 11; Barber *et al.*, 1999; Lajeunesse & St-Onge, 2008). Generally, a retreating ice margin and reduced meltwater discharge would suggest a fining upward trend (Aitken & Bell, 1998). However, in the LSEB the S3–S4 boundary is marked by a coarsening upward trend. This shows the response of the basin to the significant change in sediment provenance as fresh water tributaries became the main source of material, feeding the basin with coarse-grained particles coming from the inland (Fig. 12d).

S4–S5

This boundary corresponds to a drastic increase in grain size on the lithological log of core MD99-2220 at ~8 m beneath the seafloor. It is correlative with a fall of the RSL included in a double transgression/regression episode that occurred during Late Holocene (Fig. 3; Dionne, 2001). The origin of this episode remains poorly understood, even though it has been documented elsewhere in the world such has on the SW coast of Norway (Pirazzoli, 1991). Pirazzoli (1998) tentatively linked Late Holocene double transgression/regression events in southern Norway, western Hudson Bay and Québec to local interplays between the rate of eustatic rise and local rate of glacio-isostatic uplift. In the LSLEB, the double transgression/regression episode would have led to wave-erosion of glacio-fluvial complexes located along the St. Lawrence Estuary during transgressive stages, whereas it would have permitted the fluvial incision of successions located at the river mouths and probably also upstream the estuary during regressive stages (see Hart & Long 1996 for St. Lawrence Gulf and Estuary examples), both delivering coarse-grained material to the basin during this episode (Fig. 12d).

CONCLUSION

The LSLEB permitted to preserve a thick (up to 450 m) sedimentary succession that records at least the late stages of the Quaternary. The bedrock topography along with the sediment processes dictated the way the LSLEB was filled during the Quaternary. This topography includes two troughs that probably result from repeated episodes of glacial erosion. The larger volume of pre- to Early Holocene units within the troughs demonstrates they were efficient sediment traps. Because the troughs were located close from the front of the Laurentide Ice Sheet between 13 and 11 kyr BP, i.e. when sedimentation rates were high, they considerably reduced the transport of glacial material downstream up to the termini of the system, the Laurentian Fan. The boundary between S1 and S2 corresponds, at least locally, to an unconformity. However, the absence of geochronological control on unit 1 prevents to determine the time hiatus between units and to fully interpret the base of the succession. The bounding surfaces of S2–S8 do not suggest the presence of major hiatuses or unconformities during the late-Wisconsinan glacial and deglacial episodes, the only erosional character being related to local channel formation, mass-wasting deposition and iceberg scouring. Therefore, it reinforces the idea that the LSLEB permitted to fully preserve the late Quaternary sediment package at the regional scale. The high sedimentation rates recorded in the LSLEB are not related to eustatic fluctuations but rather to the proximity of major sediment sources (e.g. the front of the Laurentide Ice Sheet) and the capacity of these sources to deliver sediments in the basin. Moreover, sea-level variations are not first-order mechanisms in the infill history of the LSLEB. Consequently, classic sequence stratigraphy models do not apply to this basin and perhaps also to other high-latitude elongated basins in the world.

ACKNOWLEDGEMENTS

Authors would like to thank crew members of R.V. Coriolis II, CCGS Matthew and CCGS F.G. Creed. Scientific staffs of the Geological Survey of Canada, INRS-ETE, Université Laval and ISMER involved in the various scientific cruises and data analysis are also greatly acknowledged. Special thanks to M. Parent (GSC-Q) for sharing his knowledge of the Laurentide Ice Sheet with the authors and A. Smirnoff (GSC-Q) for his precious advices during the realization of the 3-D model. G. St-Onge and P. Lajeunesse also acknowledge support from the Natural Sciences and Engineering Research Council of Canada (NSERC) through ship time and discovery grants. We are grateful to Denis Lavoie (GSC-Q) for constructive remarks made on the preliminary version of the manuscript. Craig Fulthorpe, Marc De Batist, Peter van der Beek and an anonymous reviewer significantly improved the manuscript. This is Geological Survey of Canada contribution no. 20090103 and GEOTOP contribution no. 2009-0014.

REFERENCES

Aitken, A.E. & Bell, T.J. (1998) Holocene glacimarine sedimentation and macrofossil palaeoecology in the Canadian high arctic: environmental controls. *Mar. Geol.*, **145**, 151–171.

Allen, G.P. & Posamentier, H.W. (1993) Sequence stratigraphy and facies model of an incised valley fill – the Gironde Estuary, France. *J. Sediment. Petrol.*, **63**, 378–391.

Ballantyne, C.K. (2002) Paraglacial geomorphology. *Quat. Sci. Rev.*, **21**, 1935–2017.

Barber, D.C., Dyke, A., Hillaire-Marcel, C., Jennings, A.E., Andrews, J.T., Kerwin, M.W., Bilodeau, G., McNeely, R., Southons, J., Morehead, M.D. & Gagnon, J.M (1999) Forcing of the cold event of 8200 years ago by catastrophic drainage of Laurentide lakes. *Nature*, **400**, 344–348.

Bellefleur, G., Duchesne, M.J., Hunter, J., Long, B.F. & Lavoie, D. (2006) Comparison of single- and multichannel high-resolution seismic data for shallow stratigraphy mapping in the St. Lawrence River estuary. Current Research of the Geological Survey of Canada, 2006-D2, 10pp.

Bernatchez, P. (2003) Évolution littorale holocène et actuelle des complexes deltaïques de Betsiamites et de Manicouagan-Outardes: synthèse, processus, causes et perspectives. Unpublished Ph.D. Thesis, Université Laval, Québec.

Berryhill, H.L. Jr., Suter, J.R. & Hardin, N.S. (1986) Late Quaternary Facies and Structure, Northern Gulf of Mexico: Interpretation from Seismic Data. *AAPG Stud. Geol.*, **23**, 131–189.

Bolduc, A. & Duchesne, M.J. (2009) Sandy ripples, dunes and megadunes of the St. Lawrence Estuary: a dynamic system. *J. Water Sci.*, **22**, 125–134.

Bougamont, .M. & Tulacyk, S. (2003) Glacial erosion beneath ice streams and ice-stream tributaries: constraints on temporal and spatial distribution of erosion from numerical simulations of a West Antarctic ice stream. *Boreas*, **32**, 213–235.

Bromhead, E.N. (1986) *The Stability of Slopes*. Surrey University Press, New York, NY.

Campbell, D.C., Duchesne, M. & Bolduc, A. (2008) Geomorphological and geophysical evidence of Holocene seafloor instability on the southern slope of the Lower St. Lawrence Estuary, Québec. In: *Fourthth Canadian Conference on Geohazards: from Causes to Management* (Ed. by J. Locat, D. Perret, D. Turmel, D. Demers & S. Leroueil), pp. 367–374. Presse de la Université Laval, Québec.

Carignan, J., Gariépy, C. & Hillaire-Marcel, C. (1997) Hydrothermal fluids during Mesozoic reactivation of the St. Lawrence rift system, Canada: C, O, Sr and Pb isotopic characterization. *Chem. Geol.*, **137**, 1–21.

Cauchon-Voyer, G., Locat, J. & St-Onge, G. (2008) Late-Quaternary morpho-sedimentology and submarine mass movements of the Betsiamites area, Lower St. Lawrence Estuary, Quebec, Canada. *Mar. Geol.*, **251**, 233–252.

Champagnac, J.D., Molnar, P., Anderson, R.S., Sue, C. & Delacou, B. (2007) Quaternary erosion-induced isostatic rebound in the western Alps. *Geology*, **35**, 195–198.

Dalrymple, R.W., Boyd, R. & Zaitlin, B.A. (1994) Incised-Valley Systems: Origin and Sedimentary Sequences. SEPM Special Publication no. 51, Tulsa, Oklahoma.

Dionne, J.-C. (1973) La dispersion des cailloux ordoviciens dans les formations quaternaires au Saguenay/Lac-St-Jean, Québec. *Rev. Géogr. Montréal*, **27**, 339–364.

Dionne, J.-C. (1988) Holocene relative sea-level fluctuations in the St. Lawrence estuary, Québec, Canada. *Quat. Res.*, **29**, 233–244.

Dionne, J.-C. (2001) Relative-sea-level changes in the St. Lawrence Estuary from deglaciation to present day. In: *Deglacial History and Relative Sea-Level Changes, Northern New England and Adjacent Canada* (Ed. by T.K. Weddle & M.J. Retelle), pp. 271–284 *Geol. Soc. Am. Spec. Pap. 351, Boulder, Colorado*.

Dubois, J.M.M. (1980) Géomorphologie du littoral de la côte nord du St-Laurent. In: *The Coastline in Canada* (Ed. by S.B. McCann), pp. 215–238 *Geol. Surv. Canada Pap.* 80-10.

Duchesne, M.J. & Bellefleur, G. (2007) Processing of single-channel, high-resolution seismic data collected in the St. Lawrence estuary, Quebec. Current Research of the Geological Survey of Canada 2007-D1, 11pp.

Duchesne, M.J., Long, B.F., Urgeles, R. & Locat, J. (2003) New evidence of slope instability in the Outardes Bay delta area, Quebec, Canada. *Geo-Mar. Lett.*, **22**, 233–242.

Duchesne, M.J., Pinet, N., Bolduc, A., Bédard, K. & Lavoie, D. (2007) Seismic stratigraphy of the Lower St. Lawrence River estuary (Quebec) Quaternary deposits and seismic signature of the underlying geological domains. Current Research of the Geological Survey of Canada 2007-D2, 14pp.

Dupuis, L. & Ouellet, Y. (1999) Prévision des vagues dans l'estuaire du Saint-Laurent à l'aide d'un modèle bidimensionnel. *Can. J. Civil Eng.*, **26**, 713–723.

Dyke, A.S. (2004) An outline of North American deglaciation with emphasis on central and northern Canada. In: *Developments in Quaternary Science 2 – Quaternary glaciations – extent and chronology, part II. North America* (Ed. by J. Ehlers & P.L. Gibbard), pp. 373–424. Elsevier, The Netherlands.

Dyke, A.S. & Peltier, W.R. (2000) Forms, response times and variability of relative sea-level curves, glaciated North America. *Geomorphology*, **32**, 315–333.

Dyke, A.S. & Prest, V.K. (1987) Late Wisconsinan and Holocene history of the Laurentide Ice Sheet. *Géogr. Phys. Quat.*, **41**, 237–263.

Faugères, J.-C., Stow, D.A.V., Imbert, P. & Viana, A. (1999) Seismic features diagnostic of contourite drifts. *Mar. Geol.*, **162**, 1–38.

Fulthorpe, C.S., Austin, J.A., Jr. & Mountain, G.C. (2000) Morphology and distribution of Miocene slope incisions of New Jersey: are they diagnostic of sequence boundaries. *Bull. Geol. Soc. Am.*, **112**, 817–828.

Gagné, H., Lajeunesse, P., St-Onge, G. & Bolduc, A. (2009) Recent transfer of coastal sediments to the Laurentian Channel, Lower St. Lawrence Estuary (Eastern Canada), through submarine canyon and fan systems. *Geo-Mar. Lett.*, **29**, 191–200.

Gee, M.J.R., Masson, D.G., Watts, A.B. & Mitchell, N.C. (2001) Passage of debris flows and turbidity currents through a topographic constriction: Seafloor erosion and deflection of flow pathways. *Sedimentology*, **48**, 1389–1409.

Hart, B.S. & Long, B.F. (1996) Forced regressions and lowstand deltas: Canadian examples. *J. Sediment. Res.*, **66**, 820–829.

Hjelstuen, B.O., Sejrup, H.P., Haflidason, H., Nygard, A., Berstad, I.M. & Knorr, G. (2004) Late Quaternary seismic stratigraphy and geological development of the south Voring margin, Norwegian Sea. *Quat. Sci. Rev.*, **23**, 1847–1865.

Josenhans, H. & Lehman, S. (1999) Late glacial stratigraphy and history of the Gulf of St. Lawrence, Canada. *Can. J. Earth Sci.*, **36**, 1327–1345.

King, L.H. (1993) Till in the marine environment. *J. Quat. Sci.*, **8**, 347–358.

King, L.H. (1994) Proposed Younger Dryas glaciation of the eastern Scotian Shelf. *Can. J. Earth Sci.*, **31**, 401–417.

Laberg, J.S. & Vorren, O.T. (2000) Flow behaviour of the submarine glacigenic debris flows on the Bear Island Trough Mouth Fan, western Barents Sea. *Sedimentology*, **47**, 1105–1117.

Lajeunesse, P. & St-Onge, G. (2008) The subglacial origin of the Lake Agassiz-Ojibway final outburst flood. *Nat. Geosci.*, **1**, 184–188.

Lamontagne, M., Keating, P. & Perreault, S. (2003) Seismotectonic characteristics of the Lower St. Lawrence Seismic Zone, Quebec: insights from geology, magnetics, gravity, and seismics. *Can. J. Earth Sci.*, **40**, 317–336.

Lapointe, M. (2000) Late Quaternary paleohydrology of the Gulf of St. Lawrence (Québec, Canada) based on diatom analysis. *Paleogeogr. Paleoclimatol. Paleoecol.*, **156**, 261–276.

Larsson, O. & Stevens, R.L. (2008) Seismic stratigraphy of Late Quaternary deposits in the eastern Skagerrak. *Mar. Petrol. Geol.*, **25**, 1023–1039.

Lasalle, P. & Tremblay, G. (1978) Dépôts meubles du Saguenay-Lac-St-Jean. Ministère des Richesses Naturelles, Rapport Géologique 191, Québec, 61pp.

Lericolais, G., Chivas, A.R., Chiocci, F.L., Uscinowicz, S., Bo Jensen, J., Lemke, W. & Violante, R.A. (2004) Rapid transgressions into semi-enclosed basins since the Last Glacial Maximum. In 32nd IGC Florence 2004, Florence, Session 249: T05.03 – Continental shelves during the last glacial cycle 249-4.

Lin, C.-M., Zhuo, H.-C. & Gao, S. (2005) Sedimentary facies and evolution in the Qiantang River incised valley, eastern China. *Mar. Geol.*, **219**, 235–259.

Locat, J. (1977) L'émersion des terres dans la région de Baie-des-Sables/Trois-Pistoles, Québec. *Géogr. Phys. Quat.*, **31**, 297–306.

Lyså, A. & Vorren, T.O. (1997) Seismic facies and architecture of ice-contact submarine fans in high-relief fjords, Tromsø, Northern Norway. *Boreas*, **26**, 309–328.

Macgregor, K.R., Anderson, R.S., Anderson, S.P. & Waddington, E.D. (2000) Numerical simulations of glacial-valley longitudinal profile evolution. *Geology*, **28**, 1031–1034.

Mallet, J.-L. (1989) Discrete smooth interpolation. *ACM Trans. Graph.*, **8**, 121–144.

Mallet, J.-L. (1997) Discrete modeling for natural objects. *Math. Geol.*, **29**, 199–219.

Mallinson, D., Riggs, S., Thieler, E.R., Culver, S., Farrell, K., Foster, D.S., Corbett, D.E., Horton, B. & Wehmiller, J.F. (2005) Late Neogene and Quaternary evolution of the northern Albemarle Embayment (mid-Atlantic continental margin, USA). *Mar. Geol.*, **217**, 97–117.

Marshall, S.J., Tarasov, L., Clarke, G.K.C. & Peltier, W.R. (2000) Glaciological reconstruction of the Laurentide Ice Sheet: physical processes and modeling challenges. *Can. J. Earth Sci.*, **37**, 796–793.

Martineau, G. & Hocq, M. (1994) Le Quaternaire. In: *Géologie du Québec* (Ed. by C. Dubé), pp. 121–128. Les Publications du Québec, Québec.

Massé, M. (2001) Évolution générale des dépôts quaternaires sous l'estuaire du Saint-Laurent entre l'île aux Lièvres et Rimouski. Unpublished M.Sc. Thesis. Université du Québec à Rimouski, Rimouski.

Mattheus, C.R., Rodriguez, A.B., Greene, D.L Jr., Simms, A.R. & Anderson, J.B. 2007 Control of upstream variables on incised-valley dimension. *J. Sediment. Res.*, **77**, 213–224.

Mckeown, D.L. (1975) Evaluation of the Huntec ('70) Ltd. Hydrosonde deep tow seismic system. Bedford Institute of Oceanography, Dartmouth, Report Series, B1-R-75-4, 64pp.

Medvedev, S., Hartz, E.H. & Podladchikov, Y.Y. (2008) Vertical motions of the fjord regions of central East Greenland: impact of glacial erosion, deposition, and isostasy. *Geology*, **36**, 539–542.

Meigs, A. & Sauber, J. (2000) Southern Alaska as an example of the long-term consequences of mountain building under the influence of glaciers. *Quat. Sci. Rev.*, **19**, 1543–1562.

Mertz, D.F. & Gratton, Y. (1995) The generation of transverse flows by internal friction in the St. Lawrence Estuary. *Cont. Shelf Res.*, **15**, 789–801.

Mohrig, D. & Marr, J.G. (2003) Constraining the efficiency of turbidity current generation from submarine debris flows and slides using laboratory experiments. *Mar. Petrol. Geol.*, **20**, 883–899.

Montgomery, D.R. & Greenberg, H.M. (2000) Local relief and the height of Mount Olympus. *Earth Surf. Process. Landforms*, **25**, 385–396.

Mosher, D.C. & Moran, K. (2001) Post-glacial evolution of Saanich Inlet, British Columbia: results of physical property and seismic reflection stratigraphic analysis. *Mar. Geol.*, **174**, 59–77.

Neuendorf, K.K.E., Mehl, J.P. Jr. & Jackson, J.A. (2005) *Glossary of Geology*. American Geological Institute, Alexandria.

Nordfjord, S., Goff, J.A., Austin, J.A. & Sommerfield, C.K. (2005) Seismic geomorphology of buried channel systems on the New Jersey outer shelf: assessing past environmental conditions. *Mar. Geol.*, **214**, 339–364.

Nota, D.J.G. & Loring, D.H. (1964) Recent depositional conditions in the St. Lawrence River and Gulf – A reconnaissance survey. *Mar. Geol.*, **2**, 198–235.

Occhietti, S., Long, B., Clet, M., Boespflug, X. & Sabeur, N. (1995) Séquence de la transition Illinoien-Sangamonien: forage IAC-91 de l'ile aux Coudres, estuaire moyen du Saint-Laurent, Quebec. *Can. J. Earth Sci.*, **32**, 1950–1964.

Parent, M. & Occhietti, S. (1999) Late Wisconsinan deglaciation and glacial lake development in the Appalachians of southeastern Québec. *Géogr. Phys. Quat.*, **53**, 117–135.

Pelletier, J.D. (2004) Estimate of three-dimensional flexural-isostatic response to unloading: rock uplift due to late Cenozoic glacial erosion in the western United States. *Geology*, **32**, 161–164.

Pelletier, J.D. (2008) Glacial erosion and mountain building. *Geology*, **36**, 591–592.

Pinet, N., Duchesne, M., Lavoie, D., Bolduc, A. & Long, B. (2008) Surface and subsurface signatures of gas seepage in the St. Lawrence Estuary (Canada): significance to hydrocarbon exploration. *Mar. Petrol. Geol.*, **25**, 271–288.

Pirazzoli, P.A. (1991) *World Atlas of Holocene Sea-Level Changes*. Elsevier, Amsterdam.

Pirazzoli, P.A. (1998) *Sea-Level Changes: The Last 20 000 Years*. John Wiley & Sons, New York.

Popescu, I., Lericolais, G., Panin, N., Wong, H.K. & Droz, L. (2001) Late Quaternary channel avulsions on the Danube deep sea fan, Black Sea. *Mar. Geol.*, **179**, 25–37.

Rise, L., Bøe, R., Longva, O. & Olsen, H.A. (2008) Postglacial depositional environments and sedimentation rates in the Norwegian Channel off southern Norway. *Mar. Geol.*, **251**, 124–138.

Sangree, J.B. & Widmier, J.M. (1979) Interpretation of depositional facies from seismic data. *Geophysics*, **44**, 131–160.

Saucier, F.J. & Chassé, J. (2000) Tidal circulation and buoyancy effects in the St. Lawrence Estuary. *Atmosphere – Ocean*, **38**, 505–556.

Schwenk, T., Spieβ, V., Breitze, M. & Hübscher, C. (2005) The architecture and evolution of the middle Bengal Fan in vicinity of the active channel-levee system imaged by high-resolution seismic data. *Mar. Petrol. Geol.*, **22**, 637–656.

Shaw, J., Gareau, P. & Courtney, R.C. (2002) Paleogeography of Atlantic Canada 13-0 kyr. *Quat. Sci. Rev.*, **21**, 1861–1878.

Shaw, J., Piper, D.J.W., Fader, G.B.J., King, E.L., Todd, B.J., Bell, T., Batterson, M.J. & Liverman, D.G.E. (2006) A conceptual model of the deglaciation of Atlantic Canada. *Quat. Sci. Rev.*, **25**, 2059–2081.

Small, E.E. & Anderson, R.S. (1998) Pleistocene relief production in Laramide mountain ranges, western United States. *Geology*, **26**, 123–126.

St-Onge, G., Lajeunesse, P., Duchesne, M.J. & Gagné, H. (2008) Identification and dating of a key Late Wisconsinan stratigraphic unit in the St. Lawrence Estuary and Gulf (Eastern Canada). *Quat. Sci. Rev.*, **27**, 2390–2400.

St-Onge, G., Stoner, J.S. & Hillaire-Marcel, C. (2003) Holocene paleomagnetic records from the St. Lawrence Estuary, eastern Canada: centennial – to millennial-scale geomagnetic modulation of cosmogenic isotopes. *Earth Planet. Sci. Lett.*, **209**, 113–130.

Stern, T.A., Baxter, A.K. & Baxter, P.J. (2005) Isostatic rebound due to glacial erosion within the Transantarctic Mountains. *Geology*, **33**, 221–224.

Stow, D.A.V. & Piper, D.J.W. (1984) *Fine-Grained Sediments: Deep-Water Processes And Facies*. Geological Society Special Publication #15, Blackwell, Oxford.

Syvitski, J.P.M. (1989) On the deposition of sediment within glacier-influenced fjords: oceanographic controls. *Mar. Geol.*, **85**, 301–329.

Syvitski, J.P.M. & Praeg, D.B. (1989) Quaternary sedimentation in the St. Lawrence Estuary and adjoint areas, eastern Canada: an overview based on high resolution seismostratigraphy. *Géogr. Phys. Quat.*, **43**, 291–310.

Syvitski, J.P.M. & Schafer, C.T. (1996) Evidence of an earthquake-triggered basin collapse in Saguenay Fjord, Canada. *Sediment. Geol.*, **104**, 127–154.

Tremblay, A., Long, B. & Massé, M. (2003) Supracrustal faults of the St. Lawrence rift system, Quebec: kinematics and geometry as revealed by field mapping and marine seismic reflection data. *Tectonophysics*, **369**, 231–252.

Van Andel, T.H. & Perissoratis, C. (2006) Late Quaternary depositional history of the North Evvoikos Gulf, Aegean Sea, Greece. *Mar. Geol.*, **232**, 157–172.

Vincent, J.S. (1989) Quaternary geology of the southeastern Canadian shield. In: *Quaternary Geology of Canada and Groenland* (Ed. by R.J. Fulton), *Geol. Surv. Can., Geol. Can., no.1*, pp. 266–295.

Wilgus, C.K., Hastins, B.S., Posamentier, H., Van Wagoner, J., Ross, C.A. & Kendall, C.G. (1988) *Sea-Level Changes: An Integrated Approach*. SEPM Special Publication #42, Tulsa.

Manuscript received 28 January 2009; Manuscript accepted 24 November 2009.

